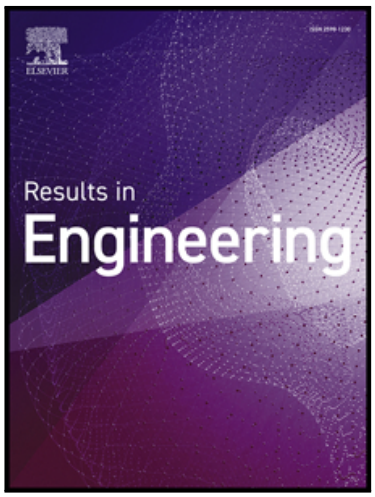

SF_6 Leakage Risk in Gas-Insulated Switchgear Under the Interaction of Ageing and Environmental Stress

Majdi M. Alomari , Ahmed Bani-Mustafa ,
Abdel-Wahab B. Dirawieh , Nafesah I. Alshdaifat , Hania EL-Kanj ,
Ayse Topal , Badriyah Alhalaili

PII: S2590-1230(26)00966-7
DOI: https://doi.org/10.1016/j.rineng.2026.109929
Reference: RINENG 109929

To appear in: *Results in Engineering*

Received date: 24 December 2025
Revised date: 28 February 2026
Accepted date: 4 March 2026

Please cite this article as: Majdi M. Alomari , Ahmed Bani-Mustafa , Abdel-Wahab B. Dirawieh , Nafesah I. Alshdaifat , Hania EL-Kanj , Ayse Topal , Badriyah Alhalaili , SF_6 Leakage Risk in Gas-Insulated Switchgear Under the Interaction of Ageing and Environmental Stress, *Results in Engineering* (2026), doi: https://doi.org/10.1016/j.rineng.2026.109929

Highlights

- Presents a stress-informed framework for assessing SF_6 leakage risk in GIS assets.
- Demonstrates limits of age-based criteria under severe environmental exposure.
- Reveals how ageing and environmental stress jointly shape emissions in hot-arid grids.
- Supports risk-based prioritisation for GIS modernisation under extreme climates.

SF_6 Leakage Risk in Gas-Insulated Switchgear Under the Interaction of Ageing and Environmental Stress

Majdi M. Alomari[1], Ahmed Bani-Mustafa[2], Abdel-Wahab B. Dirawieh[3], Nafesah I. Alshdaifat [4], Hania EL-Kanj[1], Ayse Topal[5], and Badriyah Alhalaili[6]

[1]Electrical Engineering Department, College of Engineering, Australian University (AU), Safat 13015, Kuwait
[2]Mathematics and Physics Department, College of Engineering, Australian University (AU), Safat 13015, Kuwait
[3]School of Engineering, Cardiff University, Cardiff CF10 3AT, United Kingdom
[4]JoVision, Hamburg, 22083 Germany
[5]Faculty of Economics and Administrative Sciences, Nigde Omer Halisdemir University, Nigde 51240, Turkey
[6]Kuwait Institute for Scientific Research (KISR), Safat 13109, Kuwait

Corresponding author: Majdi M. Alomari (e-mail: m.alomari@au.edu.kw)

ABSTRACT

Gas-insulated switchgear (GIS) is critical for high-voltage transmission networks but poses environmental challenges due to sulfur hexafluoride (SF_6) leakage, especially under hot-arid conditions. This study develops a unified Reliability–Environmental–Economic (REE) framework that integrates Bayesian Weibull reliability modelling under fully right-censored data, composite environmental stress decomposition, and probabilistic leakage estimation for Kuwait's 132–400 kV GIS fleet. Results indicate a weakly increasing age-dependent hazard regime ($\beta > 1$), with environmental stress (temperature, dust, salinity, and humidity) emerging as the dominant driver of leakage variability. Fleet-level analysis estimates baseline SF_6 leakage at ≈6.24 t yr^{-1} (≈1.52×10^5 t CO_2 -eq yr^{-1}, IPCC GWP100). Stress-mitigation and partial replacement scenarios reduce emissions growth but cannot eliminate long-term risk. Cooling retrofits yield moderate reductions by lowering temperature-driven stress, while partial replacement with SF_6 -free technologies achieves larger reductions by structurally removing leakage sources. Economic evaluation using discounted cash-flow analysis (3–8% rates) demonstrates that SF_6 -free replacement, despite higher upfront capital costs, achieves competitive abatement efficiency due to sustained emissions elimination over time. These findings highlight that age alone is an unreliable indicator of GIS performance. Instead, stress-informed, risk-based modernisation strategies, combining probabilistic reliability modelling, environmental exposure quantification, and economic trade-offs, are essential for effective transmission planning in hot-arid systems. The REE framework provides a transparent, data-driven basis for fleet-level screening and prioritisation, supporting Kuwait's alignment with international climate commitments and regional sustainability initiatives.

Keywords

Environmental stress factors; Gas-Insulated Switchgear (GIS); Probabilistic risk assessment; Reliability modeling; SF_6 -Free Technologies.

1. Introduction

Gas-insulated switchgear (GIS) is a core component of modern high-voltage transmission networks due to its compact design, high dielectric strength, and robustness against external contamination when compared with air-insulated alternatives [1]. The use of

sulfur hexafluoride (SF□) as the principal insulating and arc-extinguishing medium has enabled compact and reliable GIS operation, while recent international technical assessments have focused on the qualification of environmentally sustainable alternative gases capable of delivering equivalent dielectric strength and switching performance at transmission voltages [2–5].

Despite these technical advantages, SF_6 presents a significant environmental challenge. It is an extremely potent greenhouse gas with an exceptionally high 100-year global warming potential (GWP_{100} = 24,300) and an atmospheric lifetime extending over several millennia, meaning that even modest leakage rates contribute disproportionately to national and global greenhouse-gas inventories [6]. Consequently, increasing regulatory scrutiny and international climate commitments are driving global efforts to reduce or phase down SF_6 use in high-voltage equipment [7–10].

Kuwait's transmission network operates under some of the most severe environmental conditions encountered by high-voltage infrastructure worldwide. Sustained extreme ambient temperatures, coastal salinity, airborne dust, and episodic humidity spikes accelerate insulation ageing, elastomeric seal degradation, and pressure cycling within GIS enclosures [11–15]. A substantial share of the installed GIS fleet now exceeds 35–40 years of service, approaching or surpassing typical long-term operational horizons reported for transmission-level GIS installations [2,3]. Studies of similarly stressed assets indicate ageing behaviour consistent with Weibull shape parameters greater than unity, reflecting progressive degradation under sustained environmental and operational stress [16,17], even in the absence of observed end-of-life failures.

In response to environmental concerns associated with SF_6, utilities worldwide are exploring alternative insulating gases while simultaneously improving emissions monitoring, reporting practices, and asset-management strategies for existing high-voltage equipment. Engineering studies and CIGRÉ technical guidance demonstrate that clean air (F-gas-free), fluoronitrile–CO_2, and fluoroketone-based gas mixtures can achieve acceptable dielectric performance at transmission voltages up to 420 kV under controlled testing conditions [18–23]. While these technologies represent an important technical development, their long-term performance and reliability under hot-arid and coastal operating conditions remain an active area of investigation, particularly under extended validation evidence [5].

Despite extensive research on GIS reliability, environmental exposure, and SF□ emissions, these aspects are typically treated as separate analytical domains. Existing studies rarely quantify how micro-climatic stress interacts with ageing dynamics to influence leakage behaviour and fleet-level emissions under uncertainty, particularly for transmission systems operating in hot-arid environments and dominated by fully right-censored operational datasets.

This study addresses this gap by developing an integrated Bayesian–Monte Carlo Reliability–Environmental–Economic (REE) framework that links stress-adjusted reliability modelling, composite environmental stress decomposition, and physically grounded SF_6 leakage formulation within a unified probabilistic structure.

2. Literature Review

2.1. General Ageing Behaviour of Gas-Insulated Switchgear

Ageing in gas-insulated switchgear reflects the cumulative effects of dielectric stress, mechanical fatigue, and environmental exposure over multi-decade operation as documented across design, materials, and performance studies [1–4]. International technical guidance documents and industry assessments report multi-decade service performance for well-maintained transmission-level GIS and identify seal degradation, insulation deterioration, and mechanical wear as dominant degradation drivers [2,3]. As GIS assets increasingly operate beyond their original design horizons, lifetime-management studies emphasise the limitations of uniform age-based replacement criteria and the need to account for heterogeneous operating conditions [4].

Prolonged thermal and operational stress accelerates these degradation mechanisms and produces Weibull shape parameters greater than unity, indicating entry into the wear-out phase of the asset lifecycle [16,17]. Reliability assessments of SF_6 -based circuit breakers exhibit similar ageing signatures, with contact erosion and insulation decline emerging as principal contributors to hazard growth [16]. Recent reviews highlight the transition from time-based maintenance toward condition- and data-driven asset management strategies that incorporate health indices and operational context [24,25].

2.2. Environmental Stress Mechanisms in GIS Performance

Environmental exposure is a critical determinant of GIS degradation, with temperature, particulate contamination, salinity, and humidity consistently identified as major accelerants of insulation ageing and seal deterioration. Elevated temperatures reduce dielectric withstand strength, accelerate polymer relaxation, and intensify thermal cycling stresses that shorten insulation lifetime [14,15,17]. Long-term climatological analyses confirm that Kuwait experiences persistent extreme heat conditions with increasing frequency and intensity of high-temperature events [13].

Dust and airborne particulates increase surface conductivity and discharge activity, particularly in regions affected by frequent dust storms [11,15]. Coastal microclimates contribute elevated chloride aerosol concentrations that promote corrosion and modify surface electrical properties [12]. Humidity spikes, even in predominantly arid regions,

further reduce surface breakdown thresholds and exacerbate partial-discharge behaviour [14]. These mechanisms motivate the explicit inclusion of environmental stress through composite multipliers within probabilistic reliability frameworks, particularly for systems operating under extreme climatic exposure.

2.3. Modelling of SF_6 Leakage and Degradation Pathways

SF_6 leakage in GIS arises primarily from progressive deterioration of elastomeric seals, flange interfaces, and gas compartments subjected to thermal, mechanical, and pressure cycling [26–28]. Leakage rates typically below 1% per year in temperate climates can increase significantly under elevated temperatures, high internal pressures, and cyclic loading [26,27]. Empirical investigations demonstrate that leakage intensity correlates with both ageing and environmental stress, underscoring the limitations of static leakage assumptions.

CIGRÉ technical guidance highlights the sensitivity of gas density, sealing performance, and leakage behaviour to heat, humidity, and mechanical strain [22]. Advances in online diagnostics and monitoring enable linkage between leakage detection, insulation condition assessment, and ageing state, supporting more dynamic emissions evaluation [27,29].

2.4. SF_6 -Free Alternatives and Constraints of Transition in Hot-Arid Systems

Alternative insulating media, including clean air, fluoronitrile–CO_2 mixtures, and fluoroketone-based gases, demonstrate acceptable dielectric and interruption performance up to 420 kV under controlled testing conditions [18–20]. CIGRÉ Technical Brochures consolidate evidence on material compatibility, testing procedures, and application constraints for these alternatives [10, 21–23]. Early pilot installations, including climate-neutral 420 kV GIS busducts, demonstrate system-level feasibility [30].

However, no published study has yet evaluated the long-term reliability of these gases under Gulf climatic conditions characterised by extreme heat, dust exposure, and coastal salinity. This technology-validation gap directly affects transition planning in Kuwait, where environmental drivers differ substantially from those assumed in international type-testing frameworks.

2.5. Gaps in Integrated Modelling of Reliability, Environment, and Leakage

Although substantial literature exists on GIS ageing, environmental stress, leakage behaviour, and SF_6 -free technologies, these domains are rarely integrated within a single probabilistic framework. Existing models often assume rich failure data, whereas utility

datasets in Kuwait are dominated by right-censored observations and heterogeneous environmental exposure. Bayesian inference provides a robust mechanism for addressing these limitations [31,32], yet its application to GIS ageing and emissions assessment in hot-arid transmission systems remains limited.

2.6. Research Gap and Analytical Contribution

There is currently no unified framework that integrates Bayesian reliability modelling under full right-censoring, environmental stress quantification through composite multipliers (αloc), probabilistic SF□ leakage estimation, and planning-stage comparative evaluation of mitigation pathways calibrated to Gulf climatic conditions. This study addresses this gap by developing a Reliability–Environmental–Economic (REE) framework for Kuwait's 132–400 kV GIS fleet, intended as a strategic screening and prioritisation tool rather than a unit-level diagnostic or investment-optimisation model. Table 1 summarises the key studies informing the proposed Reliability–Environmental–Economic (REE) framework, covering GIS ageing mechanisms, reliability benchmarks, and thermal stress effects relevant to Kuwait's operating conditions.

Table 1. Key literature informing the Reliability–Environmental–Economic (REE) framework for GIS modernisation in hot-arid transmission systems

Reference group	Primary focus	Key contribution	Relevance to this study
[1]	GIS fundamentals	Design principles, insulation structure, operational characteristics	Technical baseline for system modelling
[2–5,10]	SF□ alternative gases and validation studies	Technical assessment, material compatibility, qualification procedures, and long-term validation evidence for SF□-free media	Technology transition baseline and performance constraints under transmission voltages
[6–9]	Climate science and regulation	Emissions impact, GWP metrics, and policy drivers	Decarbonisation and transition context
[11–15]	Environmental stressors	Effects of heat, dust, salinity, and humidity on equipment	Basis for composite α_loc stress formulation
[16,17]	Ageing and degradation modelling	Stress-dependent Weibull ageing behaviour and hazard growth	Reliability-parameter interpretation
[18–23]	Alternative gas performance testing	Experimental dielectric strength and insulation performance	Replacement scenario evaluation
[26–29]	Leakage diagnostics and monitoring	Detection, condition monitoring, and degradation indicators	Leakage-model parameterisation
[30]	Field deployment evidence	Demonstrated installation of 420 kV SF□-free GIS	Practical feasibility validation
[31,32]	Bayesian reliability methods	Inference under censored or incomplete datasets	Statistical foundation of REE framework

Together, these studies establish the empirical, environmental, and probabilistic foundations upon which the REE framework is constructed.

3. Problem Statement

Research on gas-insulated switchgear (GIS) has produced important insights into ageing mechanisms, environmental stress effects, leakage behaviour, and emerging SF_6 -free alternatives. However, these dimensions are typically analysed in isolation. Reliability studies focus on mechanical and dielectric degradation using Weibull or health-index methods, while environmental research characterises temperature, humidity, dust, and salinity impacts without integrating them into probabilistic ageing models. Likewise, leakage studies quantify emission rates but rarely link them to hazard evolution, vendor characteristics, or microclimatic stress. Economic assessments, when available, consider mitigation options but do not connect costs with changes in reliability, stress exposure, or lifecycle emissions.

In Kuwait, these limitations are particularly consequential. GIS units operate under extreme environmental conditions (persistent temperatures above 46 °C, heavy particulate loading, coastal salinity, and humidity spikes) that accelerate degradation and leakage relative to temperate systems. National SF_6 emissions have risen steadily, and many GIS units now exceed the 35–40 year service life indicated by international reliability enquiries. Yet no existing analytical framework jointly evaluates:

1. reliability degradation under right-censored operational data,
2. Kuwait-specific climatic and operational stressors,
3. stress-adjusted SF_6 leakage behaviour, and
4. indicative economic trade-offs among mitigation strategies.

The absence of such an integrated framework limits the ability of utilities to prioritise retrofit, refurbishment, and replacement actions and makes it difficult to assess the cost-effectiveness of transitions toward SF_6 -free technologies. A unified, data-driven modelling structure is therefore required to quantify how ageing, environmental stress, leakage dynamics, and economic considerations interact across multi-decade GIS lifecycles in Kuwait.

4. Research Objectives

The main objective of this study is to develop a unified Reliability–Environmental–Economic (REE) framework for Kuwait's high-voltage gas-insulated switchgear (GIS) fleet that links ageing dynamics, environmental exposure, SF_6 leakage behaviour, and mitigation pathways within a coherent probabilistic structure.

To achieve this objective, the study:

1. Calibrates a Bayesian Weibull ageing model for 485 GIS bays under full right-censoring, capturing posterior uncertainty in hazard trajectories and enabling probabilistic characterisation of degradation behaviour without reliance on observed end-of-life failures.
2. Constructs a composite environmental–operational stress coefficient (α_{total}) that integrates Kuwait-specific temperature, humidity, dust, salinity, load cycling, and vendor- and cohort-related effects, and evaluates its influence on effective lifetime and hazard evolution.
3. Develops a stress-adjusted SF_6 leakage model linking Weibull-based ageing, composite stress multipliers, and installed SF_6 inventory to estimate annual leakage at bay, substation, and system levels.
4. Implements a Monte Carlo simulation framework (n = 10,000) to propagate uncertainty in ageing, stress exposure, and leakage behaviour, and to evaluate baseline operation and alternative mitigation scenarios, including cooling retrofits and partial replacement with SF_6 -free technologies.
5. Performs a planning-stage economic comparison of mitigation pathways using emissions-abatement efficiency (cost per tonne of CO_2 -equivalent avoided) and reliability-improvement indicators, consistent with early-stage transmission modernisation and policy prioritisation.
6. Constructs a system-level risk ranking of anonymised substations by integrating stress-adjusted hazard, environmental exposure, emissions intensity, and operational context to support prioritised modernisation planning.

These objectives are designed to provide comparative, fleet-level decision support rather than final procurement or investment strategies. By isolating the technical, environmental, and reliability drivers governing SF□ leakage behaviour, the proposed framework establishes the empirical and probabilistic foundation required for subsequent project-level financial appraisal, including detailed life-cycle costing and capital-allocation analyses. Such downstream evaluations build directly on the stress-adjusted hazard and leakage characterisation developed in this study and are addressed in separate, complementary research efforts.

5. Methodology

This section outlines the integrated Reliability–Environmental–Economic (REE) framework developed to model ageing, environmental and operational stress, leakage behaviour, and modernisation pathways for Kuwait's GIS fleet. The approach combines Bayesian reliability modelling, a composite environmental stress index, stress-adjusted hazard estimation, a physically based leakage model, probabilistic emissions simulation, and an indicative economic evaluation.

Real utility data were available for 485 GIS bays across multiple voltage classes (132, 300, 400 kV) and environmental zones. All substation identifiers were anonymised, and GIS vendors were consolidated into technology families to protect confidentiality while maintaining engineering relevance.

5.1. Methodological Overview

The methodological structure of the REE framework is visually summarised in Figure 1.

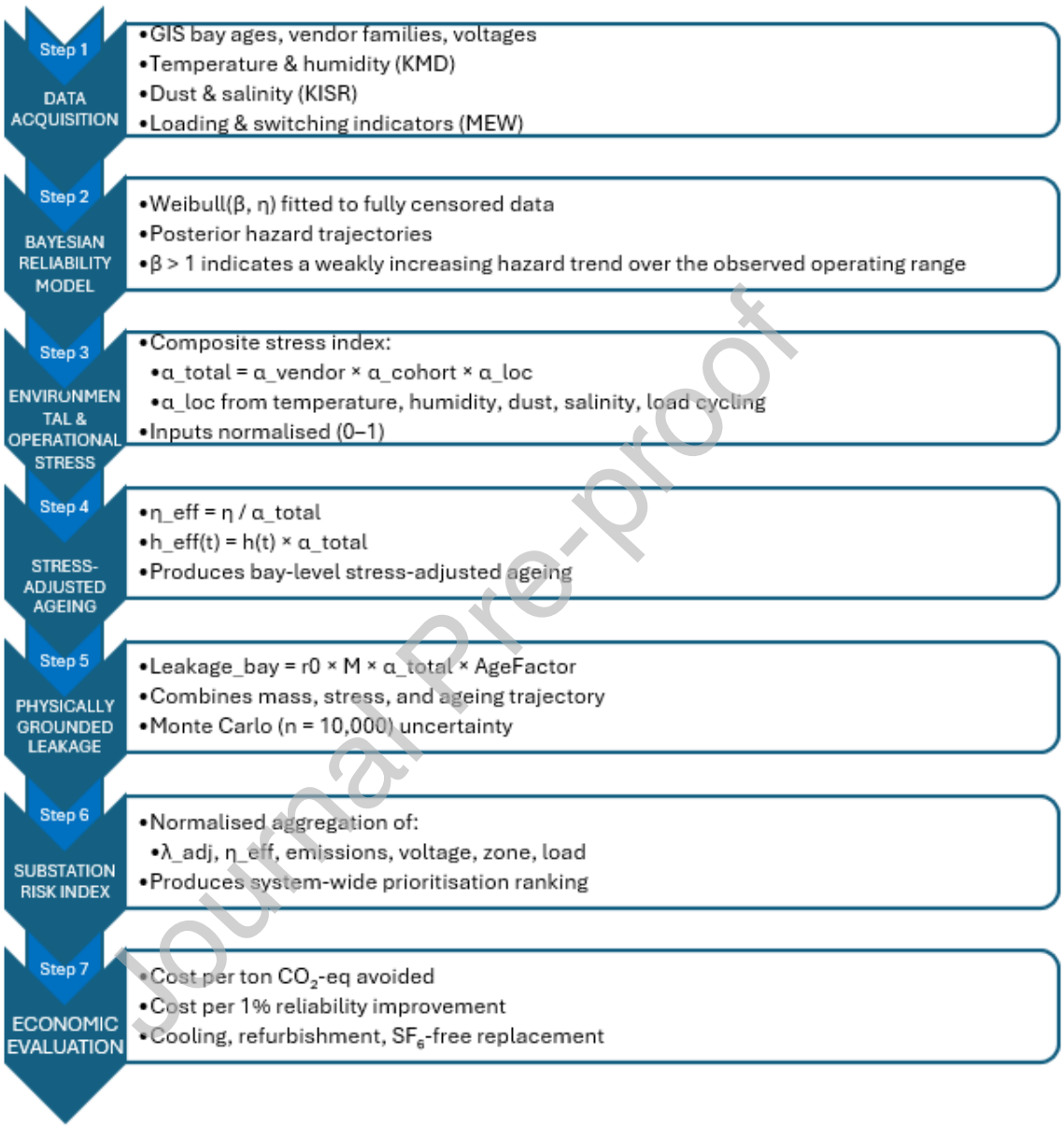

Fig. 1. Methodological Overview of the REE Framework

5.2 Reliability Modelling Framework

Ageing behaviour was modelled using a two-parameter Weibull distribution, which is widely applied to represent gradual degradation processes in high-voltage switchgear. Operational age data for 485 GIS bays were fully right-censored, as all units remain in service at the time of analysis. Bayesian inference was employed to estimate the posterior

distributions of the Weibull shape (β) and scale (η) parameters under this censored structure.

Under fully right-censored conditions, the Weibull shape parameter β is not interpreted as an empirical point estimate of failure frequency. Instead, β is treated as a probabilistic descriptor of the prevailing hazard regime relative to the threshold β = 1, which distinguishes decreasing, constant, and increasing hazard behaviour. Within the Bayesian framework, the survival of all 485 bays over the observed operating window constrains the admissible parameter space and excludes hazard trajectories inconsistent with long-term survival. This regularised interpretation follows established Bayesian reliability practice for zero-failure datasets and enables comparative hazard assessment without end-of-life prediction [33–35].

Substation identifiers were anonymised, and manufacturers were consolidated into technology families (G1–G7) after parameter estimation to preserve confidentiality without influencing statistical inference. The Bayesian formulation enables explicit representation of parameter uncertainty and avoids the need to assume hypothetical failure times, which would bias ageing estimates under full censoring.

Posterior estimates yielded values of β greater than unity, consistent with a weakly increasing age-dependent hazard over the observed operating range. Given the absence of observed end-of-life failures, η is interpreted as a normalising parameter governing relative ageing trajectories rather than as a predictor of absolute physical lifetime. Accordingly, the reliability model is used to derive comparative hazard evolution across assets, not literal replacement ages.

Weakly informative priors were applied to constrain posterior drift under full censoring. Posterior predictive validation presented in section 5.3 confirms that the fitted model reproduces the observed age distribution without inducing artificial early-life failures or implausible hazard escalation. The resulting posterior hazard trajectories form the reliability input to the stress-adjusted ageing and leakage models developed in subsequent sections.

5.3 Posterior Predictive Validation

Posterior predictive checks were performed to evaluate the adequacy of the Weibull specification under full right-censoring. Synthetic datasets were generated from posterior draws of β and η and compared with the empirical age distribution of the GIS fleet.

The replicated distributions reproduced the observed central tendency and spread across the 6–52 year operating window, with no systematic deviation in the lower or upper age ranges. Kolmogorov–Smirnov diagnostics p-value ($p > 0.05$) and posterior predictive checks (PPP ≈ 0.5) indicated satisfactory agreement between simulated and observed data. These results confirm that the Weibull model provides an adequate statistical representation of fleet-level ageing behaviour under censored conditions.

Because predictive power beyond the observed age range is inherently limited by the data structure, posterior predictive checks are interpreted as validation of internal consistency rather than as evidence of long-term lifetime accuracy. This validation supports the use of posterior hazard trajectories as relative ageing inputs to the stress-adjusted reliability and leakage formulations.

5.4 Hazard Function Characterisation

For each posterior draw, the age-dependent hazard function was computed using the standard Weibull formulation presented in Equation (1):

$$h(t) = \frac{\beta}{\eta}\left(\frac{t}{\eta}\right)^{\beta-1} \quad (1)$$

where:
β is the shape parameter governing the age dependence of the hazard.
η is the scale parameter controlling the temporal normalisation of the ageing trajectory.

Posterior estimates yielded values of $\beta > 1$, which are consistent with a weakly increasing hazard trend over the observed operating range of the fleet. Within the available data window (6–52 years), the posterior mean hazard increases gradually with age, reflecting progressive degradation rather than abrupt wear-out behaviour.

Because the dataset is fully right-censored and contains no observed end-of-life failures, uncertainty in the hazard function increases at higher ages. This uncertainty reflects posterior extrapolation rather than identifiable failure dynamics. The widening credible intervals beyond approximately 40 years therefore reflect posterior extrapolation uncertainty, not a physical transition to a failure-dominated regime. Accordingly, hazard trajectories are interpreted as relative ageing modifiers for comparative screening rather than deterministic predictors of failure timing.

These hazard functions are subsequently propagated into the stress-adjusted reliability formulation as presented in section 5.6 and the SF_6 leakage model in section 5.7, where they interact with environmental stress multipliers and equipment characteristics.

5.5 Composite Environmental and Operational Stress Index

Environmental and operational exposure is represented through a multiplicative composite stress index that scales ageing behaviour and leakage potential in a manner consistent with the physical and operational conditions of Kuwait's GIS fleet. The composite stress index is constructed for comparative scaling and prioritisation rather than for statistical inference, and its role within the REE framework is to function as a physically interpretable stress modifier rather than as an estimable latent variable.

The composite stress index is defined as:

$$\alpha_{\text{total}} = \alpha_{\text{vendor}} \times \alpha_{\text{cohort}} \times \alpha_{\text{loc}} \quad (2)$$

This deterministic formulation preserves physical interpretability while avoiding subjective weighting assumptions in stress aggregation. The vendor component, α_{vendor}, reflects systematic differences in sealing design, materials, and manufacturing practices across GIS technology families. These modifiers are derived from Ministry of Electricity and Water (MEW) technical records, inspection outcomes, and aggregated maintenance experience, and are applied comparatively rather than as absolute performance ratings. To preserve confidentiality while retaining engineering relevance, manufacturers are consolidated into anonymised technology families (G1–G7).

The cohort component, α_{cohort}, represents technology vintage and manufacturing generation. Cohorts (pre-1990, 1990–2010, post-2010) correspond to documented transitions in GIS design standards, insulation materials, and sealing technologies. This component captures relative differences in ageing sensitivity across generations without imposing discrete lifetime thresholds or deterministic replacement criteria.

The local environmental component, α_{loc}, captures spatially varying climatic and operational stressors across Kuwait, including temperature α_{T} and humidity α_{H} (Kuwait Meteorological Department), dust loading α_{D} and salinity exposure α_{S} (Kuwait Institute for Scientific Research), and load-related thermal cycling and switching duty α_{L} (MEW operational data). Each indicator is normalised to a 0–1 scale and combined deterministically to preserve relative stress intensity across substations without introducing subjective weighting.

Vendor (α_{vendor}) and cohort (α_{cohort}) modifiers represent design- and materials-driven sealing performance differences observed under comparable environmental exposure and are applied exclusively as relative scaling factors within a physically constrained stress framework. These modifiers are bounded, normalised to the fleet median, and cannot independently elevate a bay or substation into a high-risk category without concurrent ageing, SF_6 inventory, and local environmental stress. Accordingly, they do not predetermine replacement decisions and cannot dominate the resulting stress classification.

Together, these components form a dimensionless composite stress multiplier that modifies ageing trajectories and leakage behaviour within the REE framework. Uncertainty associated with environmental exposure and stress aggregation is incorporated through bounded perturbations during scenario-based Monte Carlo simulation (Section 5.7), ensuring that stress effects are propagated probabilistically rather than treated as exact quantities. Temperature effects are explicitly retained within the stress formulation through α_{T} and load-driven thermal cycling α_{L}; exclusion from the regression specification therefore does not remove thermal influence from the model but only prevents statistical multicollinearity in coefficient estimation.

5.6 Stress-Adjusted Reliability Parameters

Environmental and operational stress modifies ageing behaviour by proportionally adjusting the Weibull scale parameter. The effective lifetime parameter under stress is defined in Equation (3).

$$\eta_{\text{eff}} = \frac{\eta}{\alpha_{\text{total}}} \tag{3}$$

and the corresponding stress-adjusted hazard function is defined in Equation (4).

$$h_{\text{eff}}(t) = h(t) \times \alpha_{\text{total}} \tag{4}$$

This formulation preserves the baseline statistical structure of the Weibull ageing model while allowing environmental and operational conditions to scale degradation behaviour in a transparent manner. Higher stress levels reduce the effective scale parameter and elevate the hazard proportionally, whereas lower stress has the opposite effect.

Within the REE framework, these stress-adjusted parameters are interpreted as relative modifiers of ageing trajectories rather than as predictors of absolute failure timing. Their role is to ensure that bays exposed to higher climatic and operational stress exhibit proportionally higher ageing and leakage potential when compared under a common baseline.

5.7 Stress-Adjusted SF□ Leakage Model

SF_6 leakage is modelled at the bay level using a physically grounded, stress-adjusted formulation that links equipment ageing, environmental exposure, and installed gas inventory. The objective of this model is to estimate steady-state annual leakage behaviour consistent with long-term degradation processes, rather than to predict episodic release events.

Annual leakage for bay *i* is defined in Equation (5).

$$\text{Leakage}_i = r_0 \times M_i \times \alpha_{\text{total},i} \times \text{AgeFactor}_i \tag{5}$$

where:
r_0 is the baseline leakage coefficient under nominal reference conditions, representing steady-state fleet-average behaviour reported for transmission-level GIS. It is specified as a fixed scaling parameter rather than an estimated regression coefficient.
M_i is the nominal SF_6 mass.
$\alpha_{\text{total},i}$ is the composite stress index.
AgeFactor_i is derived from the posterior Weibull hazard trajectory.

In this formulation, $r_0$serves solely as a normalising baseline constant. Technology-generation differences are not embedded in r_0; instead, they are represented explicitly through vendor and cohort modifiers within α_{total}.

The AgeFactor term reflects the progressive increase in leakage susceptibility as sealing systems and interfaces degrade with age. Environmental variables enter the leakage formulation exclusively through the composite stress multiplier, reflecting their role as modifiers of degradation processes rather than as independent drivers of leakage in isolation. Vendor lineage and technology cohort effects are likewise incorporated through α_{total}, capturing systematic design-related differences.

Because the objective of the formulation is comparative scenario evaluation, the leakage model is constructed to preserve relative differences across assets rather than to reproduce exact absolute leakage magnitudes for individual bays.

Uncertainty in ageing parameters, stress multipliers, and SF_6 mass is propagated through the leakage model using Monte Carlo simulation, yielding probabilistic distributions of annual leakage at bay, substation, and system levels. These distributions form the emissions input for scenario evaluation and risk prioritisation in subsequent sections. Accordingly, reported emission values should be interpreted as probabilistic system-level estimates rather than deterministic measurements.

5.8 Substation Risk Index

A composite substation risk index was constructed to integrate ageing behaviour, environmental stress exposure, emissions intensity, and operational criticality for each anonymised substation–voltage–load group. The purpose of the index is comparative prioritisation across the fleet rather than absolute risk quantification.

The risk index for substation i is defined by Equation (6).

$$\text{Risk}_i = \text{norm}\left(\lambda_{\text{adj},i}, \eta_{\text{eff},i}, E_i, V_i, Z_i, L_i\right) \tag{6}$$

where:
$\lambda_{\text{adj},i}$ is the stress-adjusted hazard rate.
$\eta_{\text{eff},i}$ is the effective lifetime parameter.
E_i denotes annual SF_6 emissions.
$V_i$represents voltage class.
$Z_i$denotes environmental zone.
L_i denotes load type.

Each component is normalised to the interval $[0, 1]$ prior to aggregation to ensure comparability across substations with different physical and operational characteristics. Equal weighting is applied to all components to avoid subjective prioritisation and to preserve transparency in index construction.

Equal normalisation was intentionally adopted to preserve neutrality during the fleet-screening phase. The index is designed to identify relative risk exposure rather than consequence-weighted planning priorities. Higher-voltage substations inherently exhibit larger SF_6 inventories and higher absolute emissions potential, which are already reflected in the risk scores without imposing explicit voltage weighting.

The resulting index does not represent a probabilistic failure likelihood, economic optimisation metric, or dispatch priority. Instead, it provides a consistent, multi-dimensional ranking that highlights substations where elevated ageing stress, environmental exposure, emissions intensity, and operational context coincide. Consequence-weighted prioritisation, stakeholder preferences, and policy-driven weighting schemes are deliberately deferred to downstream planning or MCDA stages and are outside the scope of the present screening framework.

5.9 Environmental Driver Regression

To examine the internal structure of the local environmental stress component, a regression analysis was performed to decompose α_{loc} into its contributing variables, as shown in Equation (7).

$$\alpha_{\text{loc}} = \beta_0 + \beta_T \alpha_T + \beta_H \alpha_H + \beta_D \alpha_D + \beta_S \alpha_S + \beta_L \alpha_L + \varepsilon \quad (7)$$

The regression analysis presented here is not intended as an independent statistical validation of α_{loc}. Because α_{loc} is deterministically constructed from the same environmental and operational inputs, the regression serves solely as a diagnostic decomposition to illustrate the relative contribution of individual stress components rather than to establish causal or predictive relationships.

This analysis provides descriptive insight into how measured environmental and operational factors jointly shape local stress conditions across substations. Due to strong climatic co-variation in Kuwait, the predictors exhibit multicollinearity and are therefore interpreted collectively rather than individually. Temperature was excluded only from the regression decomposition to avoid statistical collinearity, but it remains explicitly incorporated in the stress formulation through the thermal stress component α_{T} and load-related thermal cycling term α_{L}, both of which directly influence leakage behaviour and ageing dynamics.

The resulting model explains a large proportion of the variance in α_{loc}. This outcome is expected and reflects the constructed nature of α_{loc}, which is deterministically derived from these same components through normalisation and aggregation. The regression therefore does not constitute statistical inference, validation, or prediction, and the magnitude of the coefficient of determination has no independent interpretive meaning.

Importantly, the regression outputs do not feed back into the computation or application of α_{loc}, which is obtained directly from measured inputs rather than estimated coefficients. The role of the regression is strictly interpretive, supporting physical understanding of

stress composition within the REE framework rather than parameter estimation or model calibration.

5.10 Bay-Level Emission Regression

To examine how ageing and environmental stress jointly influence SF_6 emissions at the bay level, a regression analysis was conducted linking estimated annual leakage to key explanatory variables derived from the REE framework. The regression equation is presented in Equation (8).

$$E_i = \gamma_0 + \gamma_1 \lambda_{\text{adj},i} + \gamma_2 \alpha_{\text{loc},i} + \gamma_3 M_i + \varepsilon_i \quad (8)$$

where:
$E_i$denotes estimated annual SF_6 emissions for bay i.
$\lambda_{\text{adj},i}$ is the stress-adjusted hazard rate.
$\alpha_{\text{loc},i}$ represents local environmental stress.
M_i is the nominal SF_6 mass.

The objective of this regression is interpretive rather than predictive, providing insight into the relative contribution of ageing, environmental exposure, and installed gas inventory to bay-level emissions. Because the dependent variable is derived from the stress-adjusted leakage formulation, the regression is not intended to establish independent causal relationships or to generate out-of-sample emission forecasts.

Regression results indicate that both stress-adjusted ageing and environmental exposure are positively associated with estimated emissions, while nominal SF_6 mass acts as a scaling factor. These relationships are consistent with the physical interpretation of leakage behaviour embedded in the REE framework and support the use of stress- and age-weighted leakage formulations for comparative analysis across the fleet.

Importantly, the regression does not influence the computation of bay-level emissions, which are obtained directly from the leakage model. Its role is confined to explanatory validation, confirming that the estimated emissions respond coherently to the principal drivers assumed in the modelling framework.

5.11 Planning-Stage Economic Comparison Framework

The economic component of the Reliability–Environmental–Economic (REE) framework is formulated as a planning-stage comparative assessment, rather than as a full lifecycle cost optimisation or project-level investment appraisal. Economic indicators are used to compare the relative emissions-abatement efficiency and reliability implications of alternative mitigation pathways under consistent assumptions, not to derive investment-optimal solutions or detailed capital-allocation strategies.

This boundary reflects the role of the REE framework within early-stage national transmission planning, where the objective is to support policy sequencing, technology

prioritisation, and phased modernisation decisions under uncertainty. At this stage, comparative economic signals are more informative than detailed lifecycle valuations, which are typically undertaken only after candidate pathways have been shortlisted for implementation.

Mitigation scenarios were defined to evaluate the comparative impacts of operational, technological, and replacement interventions on ageing behaviour, SF_6 emissions, and associated economic indicators. Scenarios were applied uniformly across the GIS fleet using identical baseline assumptions to ensure internal consistency and comparability.

Three primary scenario classes were evaluated:

- Baseline operation, representing continuation of current maintenance practices and prevailing environmental exposure conditions.
- Cooling retrofit, in which enhanced thermal management reduces the temperature-related component of local environmental stress while leaving equipment configuration unchanged.
- Partial replacement with SF_6 -free technology, targeting ageing GIS units beyond a defined age threshold and replacing them with commercially available SF_6 -free alternatives.

For each scenario, stress-adjusted ageing trajectories, leakage behaviour, and resulting emissions were simulated at both bay and substation levels using Monte Carlo propagation of parameter uncertainty. Scenario outcomes are therefore interpreted as conditional distributions rather than deterministic forecasts.

Cooling retrofit scenarios yield moderate simulated reductions in leakage and emissions by lowering the temperature-related contribution within the composite stress index, particularly at substations subject to elevated thermal exposure. Cooling retrofit measures may also yield secondary benefits by reducing the severity of other environmentally driven degradation mechanisms. Improved enclosure cooling and ventilation can lower internal temperature gradients, reduce condensation risk during humidity excursions, and indirectly limit dust adhesion and particulate accumulation on internal surfaces and sealing interfaces. These effects are not modelled as independent drivers but are captured implicitly through the reduction of the local environmental stress component within the composite stress index.

Partial replacement scenarios produce larger simulated reductions by directly eliminating SF_6 inventories and resetting ageing and stress effects for replaced assets. Differences across scenarios arise from the interaction between equipment age, environmental exposure, and intervention scope rather than from any single dominant factor.

Scenario performance is evaluated comparatively using fleet-level emissions, substation risk rankings, and planning-stage economic indicators. The analysis does not attempt to optimise intervention timing or investment portfolios. Instead, it illustrates the relative direction and magnitude of potential benefits under plausible intervention pathways,

providing a consistent basis for comparative assessment rather than prescriptive decision-making.

Economic comparison across interventions was performed using a discounted cash-flow (DCF) formulation to account for the time value of money. For each scenario, intervention costs were expressed as annualised cash flows and converted to net present value (NPV) using a baseline discount rate of 5% over a 10-year planning horizon aligned with the scenario window. In parallel, emissions reductions relative to the baseline were treated as annual flows and converted to present value (PV). Scenario cost-effectiveness is reported as a discounted abatement cost, defined as the ratio of NPV(cost) to PV(CO□-eq avoided), providing a consistent present-value basis for comparing operational retrofits and structural replacement pathways. A sensitivity check using discount rates of 3%, 5%, and 8% is also reported to demonstrate the stability of scenario ranking under plausible discounting assumptions. This discounted appraisal approach is consistent with established life-cycle costing and infrastructure asset-management practice [36–38].

5.12 Summary of the Proposed Methodology

Section 5 presents a unified methodological framework integrating Bayesian ageing estimation, composite environmental stress modelling, stress-adjusted reliability analysis, a physically grounded SF_6 leakage formulation, probabilistic emissions simulation, substation-level risk ranking, and planning-stage, discounted economic screening indicators. The framework ensures coherent propagation of uncertainty from ageing and environmental exposure through emissions and cost metrics, providing the analytical foundation for the scenario evaluation and interpretive discussion developed in Sections 7 and 8.

Throughout this study, Greek symbols denote multiplicative stress or reliability modifiers. The Weibull shape and scale parameters are denoted by $\beta$and η, respectively, with stress-adjusted hazard represented by $\lambda_{\text{adj}}(t)$. Environmental, vendor, and cohort stress components are represented by α_{loc}, α_{vendor}, and α_{cohort}, respectively, and combined into the composite stress multiplier α_{total}. SF□ inventory per bay is denoted by M, and the baseline leakage coefficient by r_0.

Regarding computational implementation and reproducibility, all probabilistic analyses were implemented using Monte Carlo simulation with 10,000 draws per scenario to ensure numerical stability of distributional estimates. Bayesian reliability models were estimated using weakly informative priors and verified for convergence through inspection of trace plots and posterior diagnostics. Sensitivity analyses were performed deterministically by perturbing key parameters within predefined bounds. Economic screening metrics were evaluated using discounted cash-flow formulations with sensitivity testing over plausible discount-rate ranges, consistent with planning-stage infrastructure appraisal practice. All simulations were executed using consistent random seeds to ensure internal reproducibility of results. Although calibrated to Kuwait's climatic conditions, the framework structure is transferable to other transmission systems through substitution of locally measured environmental and operational inputs.

6. Data and Model Inputs

This section describes the operational, environmental, and technical data used to implement the Reliability–Environmental–Economic (REE) framework for Kuwait's gas-insulated switchgear (GIS) fleet. It documents data sources, dataset composition, and key descriptive characteristics required for model implementation. All inputs are prepared in a manner consistent with the fully right-censored structure of the reliability data. Results obtained from application of the REE framework are presented in section 7.

6.1 Dataset Description and Raw Data Sources

The analytical dataset comprises operational and environmental information for 485 gas-insulated switchgear (GIS) bays operating within Kuwait's high-voltage transmission network. Data were compiled from the Ministry of Electricity and Water (MEW), the Kuwait Meteorological Department (KMD), and the Kuwait Institute for Scientific Research (KISR).

Operational and equipment attributes obtained from MEW include commissioning year, voltage class (132, 300, and 400 kV), vendor lineage and technology generation, nominal SF_6 mass per bay, substation loading category, switching-duty indicators, and geographic zone classification. Environmental exposure data include ambient temperature and relative humidity from KMD, as well as dust concentration, dust-storm frequency, and coastal salinity deposition indices from KISR. Together, these variables form the empirical basis for construction of the local environmental stress component α_{loc}within the composite stress index described in section 5.

Commissioning dates were standardised to compute equipment age without assuming end-of-life failures, consistent with the fully right-censored reliability modelling approach adopted in this study. The resulting fleet spans an operating age range of approximately 6 to 52 years across all voltage classes. The dataset is designed to support fleet-level screening and comparative modelling rather than unit-level condition diagnostics, and therefore does not include detailed maintenance-quality records or commissioning-phase defect indicators.

A summary of the age distribution by voltage class is reported in Table 2, while Figure 2 provides a graphical representation of the same distribution.

Table 2. Age distribution of GIS equipment by voltage class (n = 485).

Voltage (kV)	Count	Mean (yrs)	Median (yrs)	Min (yrs)	Max (yrs)
132	441	24.61	21	6	52
300	35	28.00	29	7	42
400	9	13.78	11	9	38

Note: Values represent observed operating ages; no end-of-life failures are recorded.

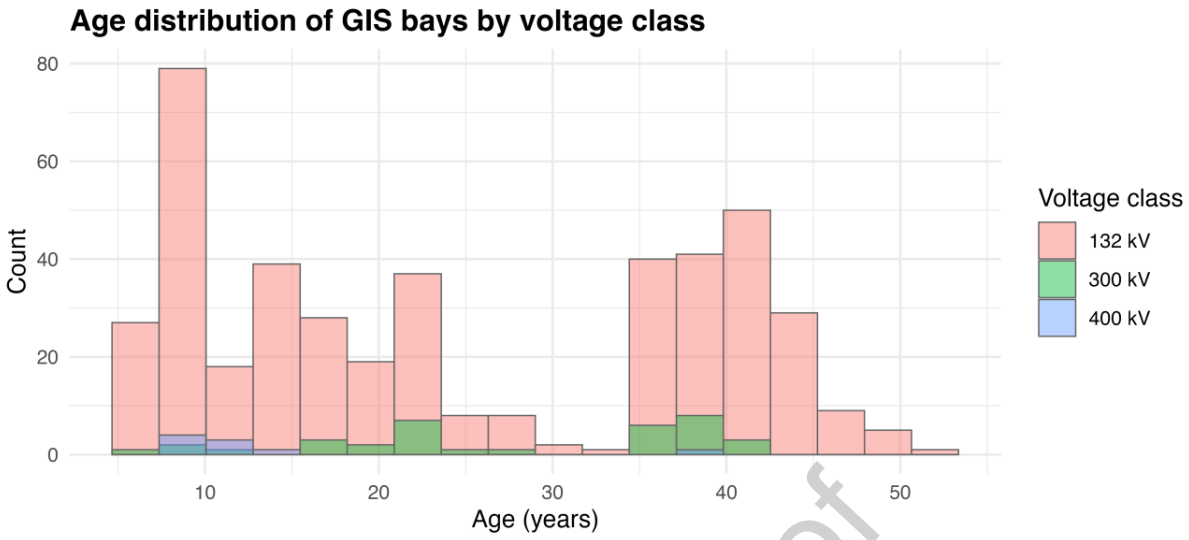

Fig. 2. Graphical Age distribution of GIS bays by voltage class

6.2 Data Cleaning and Preprocessing

Data preprocessing was performed to ensure internal consistency, traceability, and compatibility with the Bayesian reliability framework. Commissioning dates originally stored in mixed formats were standardised using deterministic parsing rules to enable consistent computation of equipment age.

All GIS bays were treated as right-censored, reflecting the absence of recorded end-of-life failures and preserving compatibility with the censored Weibull ageing model described in section 5. Vendor names and legacy brand identities were consolidated into anonymised technology families (G1–G7) to preserve confidentiality while retaining engineering relevance.

Substation identifiers were anonymised using alphanumeric labels (S001–S485), while voltage class, environmental zone, and load type attributes were retained to support stress modelling and risk assessment. Environmental indicators, including temperature, humidity, dust concentration, and salinity exposure, were maintained as continuous variables to avoid arbitrary thresholding and to preserve their physical interpretability.

No interpolation or imputation was applied to missing values. This approach is consistent with recommended practice for censored reliability datasets [29,31,35] and avoids introducing artificial information that could bias ageing or leakage estimates.

This conservative preprocessing strategy preserves the evidentiary limits of the available data and avoids introducing assumptions that could distort hazard estimation, stress attribution, or leakage behaviour under full right-censoring.

6.3 Derived Variables Used in Model Implementation

Several derived variables were constructed to link the raw operational and environmental data to the components of the REE framework.

Equipment age was computed using Equation (9) and expressed in integer years.

$$t = t_{\text{analysis}} - t_{\text{commissioning}} \tag{9}$$

Each bay was assigned to a technology cohort representing its manufacturing generation: pre-1990, 1990-2010, or post-2010. These cohorts reflect documented shifts in GIS sealing design, materials, and thermal characteristics across manufacturing periods and are used to represent relative ageing sensitivity at a comparative level, rather than discrete lifetime thresholds.

SF_6 mass per bay (M) was standardised using vendor technical documentation and MEW specification sheets. These values serve as direct inputs to the leakage model described in section 5.7.

Environmental and zone indicators were defined by associating each substation with a zone category reflecting dominant micro-environmental conditions (coastal urban, coastal industrial, urban core, inland industrial, new towns, desert remote). These indicators determine the environmental inputs used to construct the local stress component α_{loc}.

Load type categories were assigned to represent operational characteristics, including residential/urban, industrial, refinery/petrochemical, water and pumping, institutional or critical infrastructure, and renewable or transmission-related loads. These classifications feed into the load-related stress component of α_{loc}.

6.4 Model Inputs Mapped to the REE Framework

To ensure coherence between the dataset and the methodological structure, all variables were explicitly mapped to their functional roles within the REE framework. Inputs to the Bayesian reliability model described in sections 5.1 through 5.4 include equipment age t, censored survival indicators, voltage class, and technology cohort. Together, these variables determine posterior estimates of the Weibull shape and scale parameters and the corresponding age-dependent hazard functions.

Inputs to the composite environmental and operational stress index explained in section 5.5 include vendor-specific modifiers α_{vendor} derived from MEW technical assessments, cohort-based modifiers α_{cohort}, environmental variables representing temperature, humidity, dust loading, and salinity exposure, and load-related indicators capturing thermal cycling and switching duty. These inputs are combined to construct the local stress component $\alpha_{\text{loc}}$and subsequently the overall stress multiplier α_{total}.

Inputs to the SF_6 leakage model explained in section 5.7 comprise the nominal SF_6 mass per bay M, the composite stress factor α_{total}, the age-dependent hazard adjustment (AgeFactor), and the baseline leakage coefficient r_0 obtained from MEW records and engineering references. These variables jointly determine stress- and age-adjusted leakage behaviour at the bay level.

Inputs to the substation-level risk index explained in section 5.8 include the stress-adjusted hazard rate λ_{adj}, the effective lifetime parameter η_{eff}, annual leakage potential, voltage class, zone classification, load type, and environmental exposure indicators. These variables are normalised and aggregated to produce the composite risk index reported and analysed in section 7.

Economic inputs used in scenario evaluation are applied at an aggregate, planning-stage level and do not represent asset-specific cash-flow or depreciation records, consistent with the screening scope of the REE framework.

6.5 Summary of Data and Model Inputs

Section 6 documents the operational, environmental, and technical data used to implement the Reliability–Environmental–Economic (REE) framework for Kuwait's GIS fleet. All inputs were sourced from validated national datasets, anonymised for confidentiality, and processed conservatively without interpolation or imputation to preserve the fully right-censored structure required by the Bayesian reliability model.

Derived variables, including equipment age, technology cohort, nominal SF_6 mass, environmental stress indicators, and zone and load classifications, were constructed to ensure direct compatibility with the reliability, stress adjustment, leakage, and risk components of the framework. The explicit mapping of inputs to each model component ensures transparency and reproducibility and provides a coherent foundation for the results presented in section 7.

7. Results and Analysis

This section reports the results obtained from application of the probabilistic Reliability–Environmental–Economic (REE) framework to Kuwait's gas-insulated switchgear (GIS) fleet. Results are presented in a structured manner, progressing from stress-adjusted ageing and SF_6 leakage behaviour to substation-level risk ranking and scenario-based comparisons. All reported quantities are derived from the Bayesian modelling framework described in section 5 and the dataset and model inputs documented in section 6. Unless otherwise stated, results are expressed as posterior summary statistics obtained through Monte Carlo simulation.

7.1 Stress-Adjusted Leakage Structure

Annual SF_6 leakage at the bay level was estimated using the multiplicative formulation presented in Equation (10).

$$\text{Leakage}_i = r_{0,i}\, M_i\, \alpha_{\text{total},i}\, \text{AgeFactor}_i \quad (10)$$

where:
$r_{0,i}$ denotes the baseline leakage coefficient.
M_i the nominal SF_6 mass per bay.
$\alpha_{\text{total},i}$ the composite environmental and operational stress multiplier.
AgeFactor is derived from the posterior Weibull hazard trajectory.

Figure 3 presents the posterior mean hazard function with 95% credible intervals obtained from the Bayesian reliability model. Across the observed service-age range (approximately 6-52 years), the posterior mean hazard exhibits a gradual upward trend. Uncertainty increases at higher ages due to the fully right-censored nature of the dataset and the absence of observed end-of-life failures [31,32]. Consequently, the hazard tail beyond approximately 40 years should be interpreted as a model-based extrapolation rather than a prediction of physical lifetime [31,32]. In this study, the hazard function is used exclusively to scale relative ageing and leakage behaviour within the stress-adjusted framework.

Consistent with zero-failure Bayesian practice, β is interpreted here as a probabilistic indicator of hazard regime relative to the threshold β = 1 (decreasing, constant, or increasing hazard) rather than as an empirical failure-frequency estimator, and the resulting hazard trajectory is used only for comparative scaling within the REE framework [33,34].

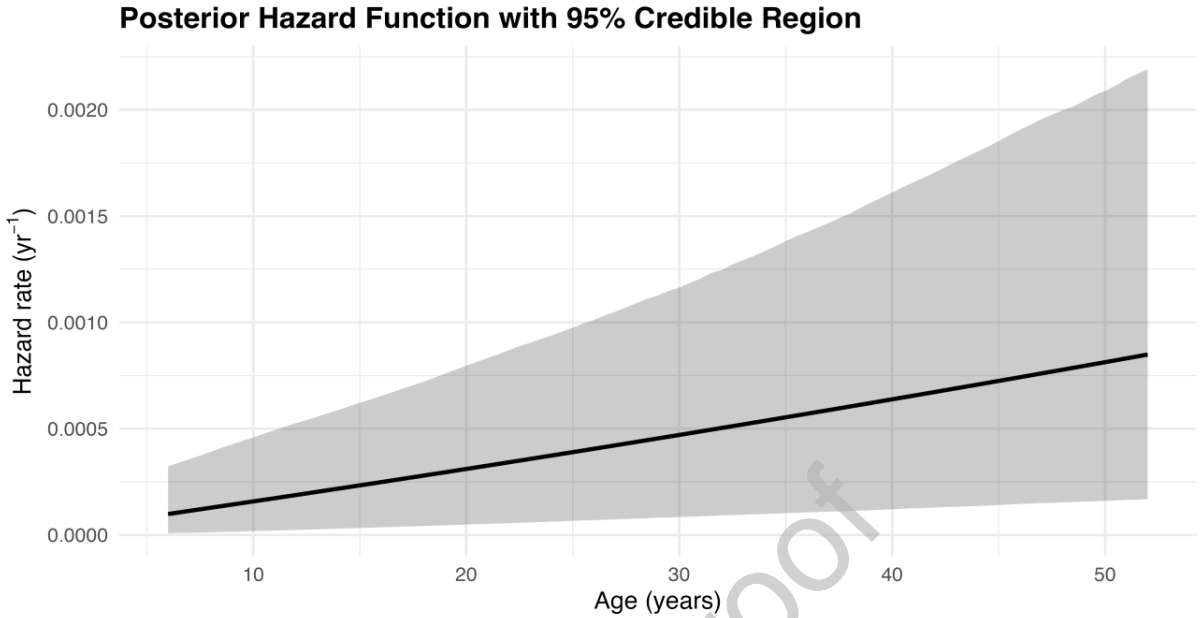

Fig. 3. Posterior Weibull hazard function with 95% credible interval.
Note: Widening uncertainty bands at higher ages reflect posterior uncertainty under full right-censoring. β is used as a hazard-regime indicator (relative to β = 1), not a failure-frequency estimator, and the hazard curve is used only for comparative scaling.

Aggregating bay-level leakage estimates yields a posterior mean baseline fleet-wide emission level of approximately 6.24 t SF□ yr⁻¹, corresponding to (≈1.52 × 10⁵ t CO□-eq yr⁻¹, IPCC GWP100) [6]. This value represents a reference condition against which scenario-based mitigation outcomes are evaluated in subsequent sections.

7.2 Vendor and Technology Effects on Composite Stress

Variation in composite environmental and operational stress across the GIS fleet was examined as a function of vendor lineage and technology generation. Differences in composite stress arise through the vendor- and cohort-specific modifiers incorporated into the REE framework and reflect how design generation interacts with Kuwait's operating environment. To avoid circular interpretation, α_{vendor} and α_{cohort} are treated as fleet-normalised scaling factors derived from documented procurement and maintenance records and applied multiplicatively alongside independently derived ageing and local stress terms; they are not subjective preference weights and cannot, on their own, determine risk classification.

Figure 4 summarises the posterior mean composite stress index α_{total} across anonymised vendor families (G1-G7). The distribution of stress multipliers shows systematic variation between vendor groups, with higher mean values observed for certain families and lower values for others. These differences reflect heterogeneity in design generation and sealing approaches as represented within the fleet-normalised scaling formulation.

Vendor families G1–G3 exhibit higher posterior mean stress multipliers relative to families G4–G7, while the latter display comparatively lower and more compact stress distributions. This pattern is consistent across Monte Carlo realisations and persists after accounting for differences in voltage class, equipment age, environmental exposure, and load characteristics. The resulting stress differentiation contributes directly to variation in stress-adjusted ageing behaviour and leakage potential at the bay level.

The composite stress index α_{total} serves as an intermediate quantity linking environmental exposure, vendor characteristics, and operational loading to the ageing and leakage processes quantified in subsequent analyses. Differences observed at the vendor-family level therefore propagate through the leakage model and influence both baseline emissions and scenario-based mitigation outcomes examined in sections 7.3 and 7.4.

Fig. 4. Posterior mean composite stress index α_{total} by vendor family (G1–G7).

7.3 Scenario-Based Emissions Distributions

Scenario-based SF_6 emissions outcomes were evaluated using Monte Carlo simulation to quantify the probabilistic impact of alternative mitigation pathways on fleet-wide leakage. For each scenario, 10,000 realisations were generated, propagating uncertainty associated with ageing behaviour, environmental stress, vendor lineage, and SF_6 inventory.

Figure 5 presents the simulated annual fleet-wide SF_6 emissions distributions under the baseline, cooling retrofit, and SF_6 -free replacement scenarios. The baseline scenario exhibits a relatively concentrated distribution centred on the posterior mean reference level reported in section 7.1, reflecting the combined effects of heterogeneous bay characteristics under unchanged operating conditions.

Under the cooling retrofit scenario, the emissions distribution shifts toward lower values relative to the baseline. The reduction is accompanied by a modest narrowing of the

distribution, indicating decreased variability in fleet-wide emissions as local environmental stress multipliers are reduced at targeted substations. The overall shape of the distribution remains unimodal, with overlap between baseline and cooling retrofit outcomes reflecting uncertainty in the magnitude and spatial extent of stress reduction.

The SF_6 -free replacement scenario yields the lowest emissions distribution among the evaluated cases. The distribution is characterised by both a reduced mean and a narrower spread compared with the baseline and cooling retrofit scenarios. This reflects the structural removal of leakage sources associated with older GIS units within the simulation horizon. Residual emissions arise from the remaining SF_6 -containing equipment retained under the scenario assumptions. Across all scenarios, differences in emissions distributions arise from the combined effects of stress modification, equipment replacement thresholds, and uncertainty in ageing and environmental exposure. These probabilistic distributions form the quantitative basis for subsequent comparison of mitigation effectiveness and economic screening outcomes.

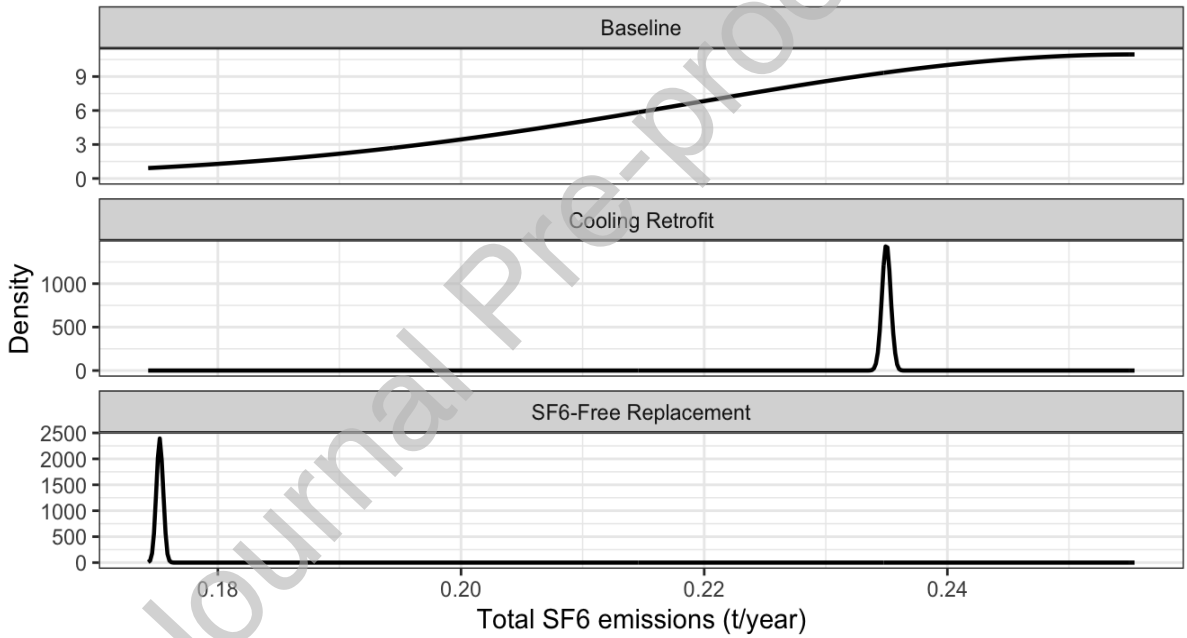

Fig. 5. Simulated annual fleet-wide SF_6 emissions distributions (n = 10,000) under baseline, cooling retrofit, and SF_6 -free replacement scenarios.

7.4 Sensitivity Analysis

A global sensitivity analysis was conducted to quantify the influence of key model parameters on annual fleet-wide SF_6 emissions. Each parameter was independently perturbed by ±20% around its baseline value, while all other inputs were held constant. The analysis was performed within the Monte Carlo framework to ensure consistency with the probabilistic structure of the REE model.

Table 3 reports the resulting changes in annual SF_6 emissions under each parameter perturbation. Variations in the composite stress index α_{total}, nominal SF_6 mass per bay M, and the baseline leakage coefficient $r_0$produce the largest absolute changes in emissions outcomes. Perturbations in the Weibull shape parameter β and scale parameter η yield smaller changes over the examined range.

The relative ranking of parameters in Table 3 reflects their contribution to variability in simulated emissions outcomes under the specified perturbation bounds. Additional testing shows that a ±10% variation in r_0 produces an approximately proportional change in absolute fleet-wide emissions while preserving relative rankings, confirming that r_0 functions as a global scaling coefficient rather than a structural driver. These results provide a quantitative basis for assessing parameter influence within the REE framework and inform the interpretation of uncertainty propagation discussed in subsequent sections. Sensitivity results confirm that SF_6 inventory and α_{loc}-driven stress dominate emissions variability, while vendor and cohort terms act as secondary modifiers that refine, rather than dictate, relative rankings. Because r_0 functions as a fleet-level scaling parameter, uncertainty in its absolute value affects magnitude but does not alter comparative risk conclusions.

Table 3. Sensitivity of annual SF_6 emissions (t yr^{-1}) to ±20% parameter perturbations

Parameter	–20%	+20%	Range	Ranking
$\boldsymbol{\alpha_{\text{total}}}$	0.214	0.296	0.082	1
$\boldsymbol{M}$	0.205	0.305	0.100	2
$\boldsymbol{r_0}$	0.224	0.286	0.062	3
$\boldsymbol{\beta}$	0.242	0.271	0.029	4
$\boldsymbol{\eta}$	0.244	0.267	0.023	5

7.5 Distribution Shape and Uncertainty Characteristics

The probabilistic structure of the Monte Carlo simulations allows direct examination of the shape and dispersion of fleet-wide SF_6 emissions outcomes under each evaluated scenario. Differences in distribution shape and uncertainty reflect the combined influence of ageing behaviour, stress modification, and structural changes to the fleet composition.

Under baseline conditions, the simulated emissions distribution exhibits relatively limited dispersion, consistent with aggregation across a large number of bays operating under similar ageing regimes. The cooling retrofit scenario shows a reduction in distribution spread relative to the baseline, indicating decreased variability in emissions outcomes as local environmental stress multipliers are reduced at selected substations.

The SF_6 -free replacement scenario produces the narrowest emissions distribution among the evaluated cases. This reduced dispersion arises from the structural removal

of leakage contributions associated with older GIS units, leading to lower variability in aggregate fleet-wide emissions within the simulation horizon.

Across all scenarios, emissions uncertainty reflects the interaction between stress adjustment, SF_6 inventory, and ageing-related factors. The relative differences in distribution width observed here are consistent with the parameter sensitivity patterns reported in section 7.4 and provide context for the emissions trajectories examined in section 7.6.

7.6 Emission Trajectories (2025–2035)

Projected fleet-wide SF_6 emissions were evaluated over the 2025–2035 horizon to examine the temporal evolution of emissions under alternative mitigation pathways. Projections were generated using the probabilistic Reliability–Environmental–Economic (REE) framework, with uncertainty propagated through Monte Carlo simulation. Results are reported using posterior mean trajectories with associated percentile envelopes to characterise the range of plausible outcomes.

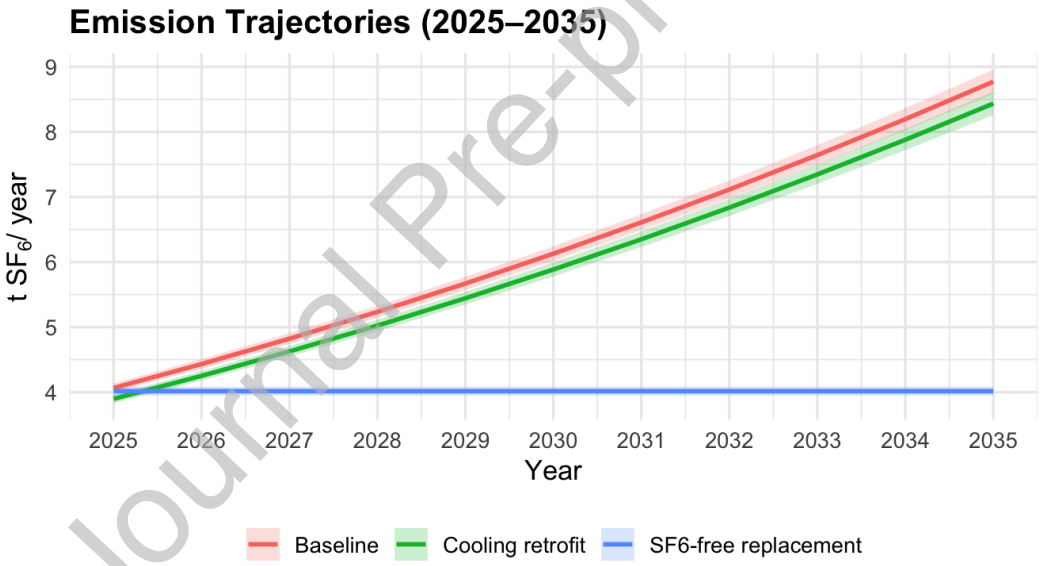

Fig. 6. Annual fleet-wide SF_6 emission projections for baseline, cooling retrofit, and SF_6 -free replacement scenarios.

Figure 6 presents the projected annual fleet-wide SF_6 emissions under the baseline, cooling retrofit, and SF_6 -free replacement scenarios. Shaded bands represent the 5th–95th percentile range across Monte Carlo simulations.

Under baseline conditions, emissions exhibit a steady upward trend across the projection horizon, reflecting the cumulative effect of ageing within an unchanged SF_6 -containing asset base. As equipment continues operation beyond its initial design period, stress-adjusted ageing leads to progressively higher leakage rates at the fleet level.

The cooling retrofit scenario moderates this growth relative to the baseline. Emissions continue to increase over time, but at a reduced rate, indicating that thermal stress mitigation slows leakage escalation without eliminating the underlying SF_6 inventory. Residual growth persists because ageing continues in non-retrofitted assets and stress reduction does not address structural leakage mechanisms.

In contrast, the SF_6 -free replacement scenario yields a substantially lower and stabilised emissions trajectory across the full horizon. Once SF_6 -containing equipment is replaced, emissions no longer increase with age, resulting in a near-constant fleet-wide leakage profile. The absence of a late-horizon rebound reflects the progressive phase-out of SF_6 inventory rather than reliance on stress mitigation alone. Emissions remain consistently well below those observed under both the baseline and cooling retrofit scenarios.

Differences between scenarios become increasingly pronounced toward the latter part of the projection horizon, highlighting the cumulative advantage of structural replacement over incremental mitigation. These trajectories provide temporal context for the comparative mitigation performance and cost-effectiveness metrics reported in Section 7.10.

7.7 Environmental Driver Effects on the Local Stress Component

Because the local stress component α_{loc} is deterministically constructed from environmental and operational drivers, the regression analysis presented in this section is intended as a decomposition of driver contributions rather than as an inferential or predictive model. The contribution of individual environmental and operational drivers to the local stress component α_{loc} was quantified using a regression-based analysis. Due to collinearity between ambient temperature and relative humidity, temperature was excluded from the regression specification. All remaining drivers were retained as continuous variables.

Table 4 reports the estimated regression coefficients, standard errors, test statistics, and goodness-of-fit metrics. The fitted model explains a large proportion of the variance in α_{loc}, which is expected given that α_{loc} is deterministically constructed from these same drivers; the regression therefore serves as a diagnostic decomposition of stress contributions rather than an inferential or predictive model.

Estimated coefficients for relative humidity (α_{H}) and load-related thermal stress (α_{L}) are positive, while coefficients associated with dust (α_{D}) and salinity (α_{S}) are negative under the adopted normalisation and aggregation scheme over the observed range. All reported coefficients are statistically significant at conventional levels. The sign and magnitude of the coefficients reflect the direction and relative scale of association between each driver and the constructed stress component within the REE framework. Although the regression is not intended for variable selection, the relative coefficient magnitudes indicate that humidity and load-related thermal stress dominate variability within the constructed index, while dust and salinity act as secondary modifiers. This suggests that

future simplified screening formulations could prioritise dominant drivers without materially altering relative stress patterns.

Table 4. Regression summary for drivers of the local stress component α_{loc}.

Variable	Coefficient	Std. Error	t-Statistic	p-Value
Intercept	−0.283	0.030	−9.45	<0.001
α_H	1.410	0.026	53.77	<0.001
α_L	0.765	0.041	18.47	<0.001
α_D	−0.106	0.049	−2.14	0.032
α_S	−0.800	0.031	−25.91	<0.001
Model R^2	0.9975	—	—	—

The high coefficient of determination ($R^2 = 0.9975$) is expected because $\alpha_{loc}$is constructed directly from the same environmental inputs; accordingly, the regression is interpreted as an explanatory decomposition rather than an inferential or predictive validation and therefore carries no independent statistical interpretive meaning.

Figure 7 presents the regression-derived importance of environmental components corresponding to the standardised regression coefficients (α_T, α_H, α_D, α_S), providing a normalised comparison of driver contributions to variation in the composite stress index α_{loc}.

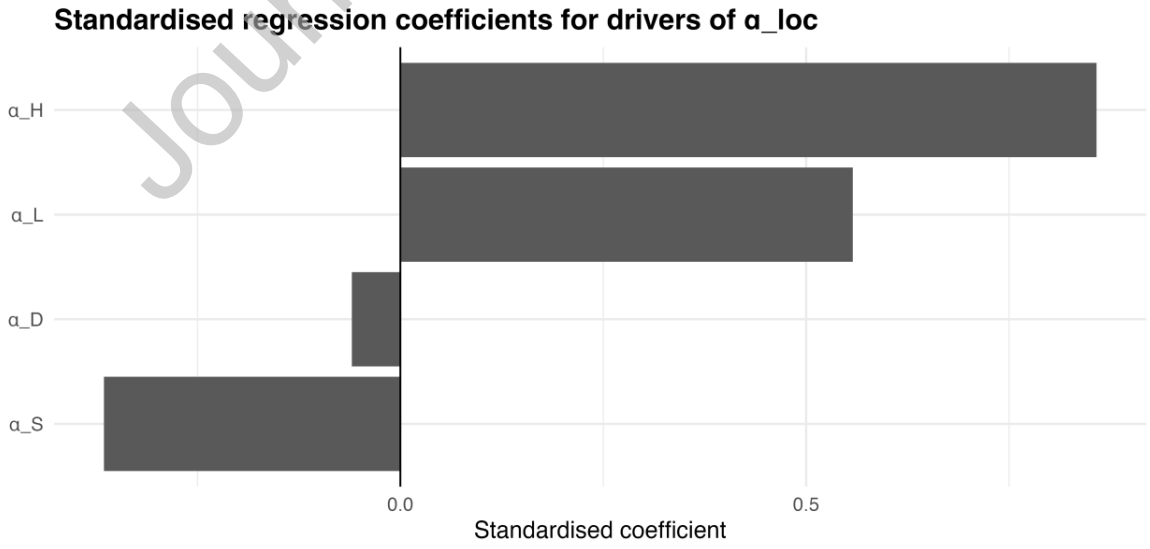

Fig. 7. Standardised regression coefficients for drivers of α_{loc}. Temperature is excluded from the regression visualisation due to collinearity with humidity; thermal effects remain incorporated in the composite stress formulation through α_T and load-driven thermal cycling terms.

7.8 Bay-Level Emission Patterns

Bay-level SF_6 emissions exhibit substantial variability across the fleet due to differences in equipment characteristics and operating conditions. Analysis of simulated bay-level outcomes indicates that environmental variables alone explain a limited fraction of the variance in annual emissions when considered in isolation.

Regression diagnostics show that variation in bay-level emissions is primarily associated with the combined influence of nominal SF_6 mass per bay, ageing behaviour encoded through the stress-adjusted hazard function, vendor lineage, and the composite stress multiplier. When these factors are considered jointly within the REE framework, substantially greater explanatory power is achieved compared with models relying solely on environmental classification.

The observed dispersion in bay-level emissions underscores the importance of a multiplicative modelling structure that integrates ageing, inventory, and stress effects rather than attributing emissions outcomes to single drivers. These patterns motivate the aggregation and prioritisation analyses presented in the subsequent subsection.

7.9 Substation Risk Index and Prioritisation

A composite substation risk index was constructed to aggregate stress-adjusted ageing behaviour, emissions potential, and contextual operational attributes at the substation level. The index combines the stress-adjusted hazard rate, effective lifetime parameter, annual SF_6 leakage potential, voltage class, environmental zone, and load type into a single normalised metric, as defined in section 5.8 .

Based on this index, GIS substation sections were ranked across the fleet. The Top-100 highest-risk sections were selected for focused analysis to characterise the distribution of technical and environmental risk across voltage classes and operating contexts. Selection was based solely on the composite risk score and does not imply operational thresholds or intervention decisions, consistent with the use of asset-management indices as screening and prioritisation tools rather than decision rules [24]. Although voltage class is not consequence-weighted within the screening index, extra-high-voltage sections remain concentrated in the upper tail of the ranking because higher-voltage GIS typically carries larger SF_6 inventories and higher stress-adjusted hazard exposure, which are embedded in the physical drivers of the risk score.

Table 5 summarises the distribution of the Top-100 highest-risk GIS sections by voltage class. The majority of high-risk sections are associated with 132 kV substations, reflecting their numerical dominance within the fleet, while higher-voltage classes account for a smaller share of the ranked subset.

Table 5. Distribution of Top-100 highest-risk GIS sections by voltage class.

Voltage (kV)	Count	Percentage (%)
132	60	60.0
300	32	32.0
400	8	8.0
Total	100	100.0

The top 15-highest-ranked individual GIS sections are reported in Table 6 using anonymised identifiers. For confidentiality and system security, only voltage class, zone classification, load type, and the normalised risk index $R_i$are presented. Absolute risk values are not reported; rankings are preserved through normalisation.

Table 6. Top-15 highest-risk anonymised GIS sections

Rank	Anonymised ID	Voltage (kV)	Zone	Load Type	Normalised Risk Index R_i
1	S001-400	400	Inland Industrial	Industrial	1.00
2	S002-400	400	Coastal Urban	Commercial / Mixed	0.689
3	S003-400	400	New Towns	Development / New Towns	0.579
4	S004-400	400	New Towns	Development / New Towns	0.579
5	S005-400	400	New Towns	Development / New Towns	0.579
6	S006-400	400	New Towns	Development / New Towns	0.579
7	S007-400	400	New Towns	Development / New Towns	0.579
8	S008-300	300	Coastal Industrial	Refinery / Industrial	0.544
9	S009-300	300	Coastal Industrial	Refinery / Industrial	0.497
10	S010-300	300	Coastal Industrial	Refinery / Industrial	0.497
11	S011-300	300	Coastal Urban	Commercial / Mixed	0.476
12	S012-300	300	Coastal Urban	Commercial / Mixed	0.476
13	S013-300	300	Coastal Urban	Commercial / Mixed	0.476
14	S014-300	300	Coastal Industrial	Refinery / Industrial	0.471
15	S015-300	300	Inland Industrial	Industrial	0.460

7.10 Scenario Comparison and Mitigation Metrics

Scenario outcomes were compared using aggregated emissions and discounted cost-effectiveness metrics to assess the relative mitigation performance of the evaluated pathways. Consistent with the revised economic framework (Section 5.11), scenario costs and emissions reductions were evaluated on a present-value basis using discounted cash-flow (DCF) analysis. Table 7 reports posterior mean annual SF_6 and CO_2 -eq outcomes and the associated discounted abatement cost under the baseline 5% discount rate and 10-year planning horizon. Table 8 summarises the sensitivity of present-value outcomes to alternative discount rates (3%, 5%, and 8%). All values are derived from Monte Carlo simulations.

Table 7. Discounted cost-effectiveness comparison of mitigation scenarios (baseline discount rate 5%, 10-year horizon).

Scenario	SF_6 emissions (t/yr)	CO_2 -eq (t/yr)	Reduction vs baseline (%)	Annualised intervention cost (KD/yr)	NPV(cost), 5% (KD)[a]	Annual CO_2 -eq avoided (t/yr)	PV(CO_2 -eq avoided), 5% (t)[b]	Discounted abatement cost (KD/tCO_2 -eq)[c]
Baseline	6.24	142,887	0.00	—	—	—	—	—
Cooling retrofit	5.19	118,824	16.84	461,364	3,562,531	24,063	185,808	19.17
SF_6 -free replacement	4.60	105,527	26.35	681,818	5,264,818	37,360	288,484	18.25

Notes: a) NPV(cost) is computed from the annualised scenario cost using a 5% discount rate over 10 years.
b) PV(CO_2 -eq avoided) is computed from annual CO_2 -eq avoided relative to the baseline using the same discount rate and horizon.
c) Discounted abatement cost is defined as NPV(cost) / PV(CO_2 -eq avoided).
d) CO_2 -eq values and scenario emissions correspond to the outputs reported in this section; the baseline scenario is the reference case.

The use of discounted present-value metrics follows standard public-sector and infrastructure appraisal guidance, in which near-term capital expenditure is weighted more heavily than deferred operational savings, consistent with life-cycle costing and government appraisal practice [36, 38].

Table 8. Sensitivity of present-value results to discount-rate selection (3%, 5%, 8%; 10-year horizon).

Discount rate	Scenario	Annualised cost (KD/yr)	NPV(cost) (KD)	Annual CO_2 -eq avoided (t/yr)	PV(CO_2 -eq avoided) (t)	Discounted abatement cost (KD/tCO_2 -eq)
3%	Cooling retrofit	461,364	3,935,529	24,063	205,262	19.17

3%	SF_6 -free replacement	681,818	5,816,046	37,360	318,688	18.25
5%	Cooling retrofit	461,364	3,562,531	24,063	185,808	19.17
5%	SF_6 -free replacement	681,818	5,264,818	37,360	288,484	18.25
8%	Cooling retrofit	461,364	3,095,790	24,063	161,465	19.17
8%	SF_6 -free replacement	681,818	4,575,054	37,360	250,689	18.25

Note: NPV(cost) and PV(CO_2 -eq avoided) are computed over 10 years using the stated discount rate; discounted abatement cost is calculated as NPV(cost) / PV(CO_2 -eq avoided).

Across the tested discount-rate range, present values vary as expected, while the relative ordering of discounted abatement cost remains stable, reflecting the use of annualised cost streams and proportional emissions reductions. This stability supports the robustness of the comparative economic screening.

Under baseline conditions, fleet-wide emissions increase over the planning horizon due to stress-adjusted ageing of the remaining SF_6 -containing asset base. Cooling retrofits reduce emissions by moderating the temperature-related contribution to local stress, yielding moderate but persistent reductions without eliminating SF_6 inventory. In contrast, SF_6 -free replacement produces the lowest emissions trajectory by structurally removing leakage sources and resetting ageing exposure for replaced units.

Discounting explicitly penalises capital-intensive replacement strategies relative to retrofit measures; however, SF_6 -free replacement remains competitive on a discounted abatement-cost basis due to sustained emissions reductions over the analysis horizon, reinforcing its role as a long-term mitigation pathway within a phased modernisation strategy.

7.11 Summary of Results

Section 7 reports the quantitative outcomes of the Reliability–Environmental–Economic (REE) framework applied to Kuwait's GIS fleet. Stress-adjusted ageing and leakage modelling indicates a baseline fleet-wide SF_6 leakage of approximately 6.24 t yr (≈1.52 × 10^5 t CO_2 -eq yr^{-1}, with emissions governed by the combined effects of equipment age, SF_6 inventory, vendor lineage, and environmental stress.

Scenario-based Monte Carlo analysis reveals systematic differences in emissions distributions and temporal trajectories across the evaluated pathways. Environmental hardening interventions (represented by the cooling-retrofit scenario) reduce both the mean and dispersion of emissions relative to baseline conditions by approximately 16–17%, reflecting mitigation of composite environmental stress rather than structural removal of SF_6 inventory. In contrast**,** SF_6 -free replacement yields the largest and most persistent emissions reduction, lowering annual fleet-wide emissions by approximately 26–31% relative to baseline conditions over the 2025–2035 planning horizon, with the narrowest uncertainty envelope.

Sensitivity analysis identifies the composite stress index α_{total} and nominal SF_6 mass per bay as the dominant contributors to emissions variability, while Weibull ageing parameters exert a secondary influence within the examined bounds. This confirms that emissions behaviour is primarily governed by physical inventory and environmental exposure rather than by statistical ageing uncertainty alone. Regression-based decomposition of the local stress component shows strong associations with humidity and load-related thermal stress, with dust and salinity acting as secondary but non-negligible contributors under Kuwait's climatic conditions. The high coefficient of determination reflects deterministic index construction rather than inferential causality.

At the substation level, aggregation of stress-adjusted ageing, emissions intensity, and contextual operational attributes produces a ranked composite risk index that consistently identifies a limited subset of high-risk GIS sections across voltage classes. Although voltage class is not explicitly weighted within the screening index, extra-high-voltage substations systematically appear among the highest-risk assets due to larger SF_6 inventories and elevated stress-adjusted hazard exposure.

Comparative mitigation metrics demonstrate clear trade-offs between intervention pathways. Discounted economic screening indicates that cooling retrofits offer moderate emissions abatement with lower near-term financial burden, while SF_6 -free replacement remains competitive on a discounted abatement-cost basis despite higher upfront capital requirements. These findings confirm that incremental environmental hardening and structural replacement play complementary roles in phased transmission-network decarbonisation strategies.

Together, these results provide a coherent probabilistic characterisation of ageing behaviour, emissions dynamics, uncertainty structure, and mitigation trade-offs under extreme climatic exposure. The implications for policy design, capital-allocation strategy, and phased GIS modernisation under Kuwait's operating conditions are discussed in Section 8.

8. Discussion

This study developed and applied an integrated Reliability–Environmental–Economic (REE) framework to examine ageing behaviour, environmental stress, leakage dynamics, and mitigation pathways for Kuwait's high-voltage gas-insulated switchgear (GIS) fleet. Unlike temperate transmission systems, Kuwait's GIS fleet operates under sustained ambient temperatures exceeding 45 °C, frequent dust storms, and coastal salinity, conditions under which seal ageing and pressure cycling dominate leakage behaviour. These findings are consistent with earlier planning-level analyses conducted for Kuwait's transmission network [39], while providing a deeper probabilistic interpretation of ageing–environment interactions. This section interprets the probabilistic results presented in Section 7 in relation to Kuwait's operating environment and the methodological objectives defined in Section 4, without reiterating numerical outcomes already reported.

8.1 Interpretation of Stress-Adjusted Ageing and Leakage Behaviour

The stress-adjusted reliability analysis indicates that the GIS fleet predominantly operates within a wear-out–dominated hazard regime, consistent with a population containing a substantial share of assets exceeding three decades of service. Within a censored-data Bayesian Weibull setting, this manifests as $\beta > 1$ indicating an increasing hazard regime rather than an empirically observed failure-rate trend [31–35]. Under full right-censoring, the Weibull-based formulation does not yield deterministic end-of-life predictions; instead, it characterises relative ageing tendencies and sensitivity to stress. Accordingly, the Weibull shape parameter is interpreted as an indicator of the prevailing hazard regime ($\beta > 1$) rather than as an empirical failure-rate estimator. This interpretation is consistent with established Bayesian reliability practice for high-reliability infrastructure operating under zero-failure or heavily censored conditions [33–35]. Leakage behaviour emerges from the interaction between ageing state and local environmental and operational stress. Elevated stress levels increase leakage potential primarily when they coincide with older equipment generations, vendor-specific sealing characteristics, and larger SF_6 inventories. This interaction explains why emissions are concentrated within a limited subset of GIS bays rather than being uniformly distributed across the fleet. Environmental stress therefore acts as an amplifier of ageing-driven degradation, rather than as an independent leakage mechanism, reinforcing the need for integrated modelling approaches [24,25].

8.2 Environmental Drivers and Vendor-Related Heterogeneity

Regression-based decomposition of the local stress component α_{loc}demonstrates strong associations with relative humidity and load-related thermal stress over the observed operating range. These associations are consistent with known degradation mechanisms in sealed GIS systems exposed to sustained thermal cycling and moisture ingress. The very high coefficient of determination reflects the deterministic construction of $\alpha_{loc}$from these same variables and should therefore be interpreted strictly as a diagnostic decomposition rather than inferential validation, consistent with best practice for composite indices.

Vendor lineage introduces an additional layer of heterogeneity through differences in design generation, sealing approaches, and materials performance. Vendor- and cohort-related modifiers act as secondary scaling factors rather than dominant drivers of risk, as confirmed by sensitivity analysis showing the primary influence of SF_6 inventory and environmental stress. This interaction-based structure avoids circular reasoning and aligns with asset-management literature that treats manufacturer lineage as a contextual modifier rather than a primary determinant of failure or replacement decisions [24].

8.3 Integrated Interpretation of Scenario Outcomes and Uncertainty

The REE framework integrates stress-adjusted ageing, emissions estimation, and uncertainty propagation within a single probabilistic structure. Scenario analysis reveals distinct mitigation mechanisms across the evaluated pathways**.** Cooling retrofits primarily

reduce local stress intensity, leading to moderate reductions in emissions and associated uncertainty.

Although labelled “cooling retrofit” for brevity, this scenario is implemented as a proportional reduction in the composite local stress term α_{loc}, which explicitly incorporates humidity, dust loading, and salinity exposure in addition to temperature. This preserves the physical thermodynamic mechanism while avoiding statistical collinearity in regression diagnostics. It therefore represents a broader environmental hardening intervention rather than a purely thermal measure, consistent with contamination-mapping and insulation-coordination practice reported in the CIGRÉ literature [2–4] [21–23]. SF_6 -free replacement reduces emissions by structurally eliminating leakage pathways, producing larger reductions and narrower uncertainty envelopes over time. Sensitivity analysis confirms that emissions outcomes are governed primarily by stress amplification and SF_6 inventory, while ageing parameters exert a secondary influence under fully right-censored data.

8.4 Asset-Level Prioritisation, Voltage Criticality, and Risk Aggregation

Aggregation of stress-adjusted ageing behaviour, leakage potential, and contextual operational attributes into a composite risk index enables consistent fleet-wide screening. Although voltage class is not explicitly weighted, higher-voltage substations inherently carry larger SF_6 inventories and greater absolute emissions potential. As a result, 300–400 kV assets systematically emerge among the highest-risk sections through physical drivers rather than imposed weighting.

This screening-first philosophy aligns with modern asset-management practice, where neutral indices are used to identify candidate assets prior to consequence-weighted or MCDA-based prioritisation in downstream planning stages [24,40].

8.5 Economic Interpretation and Budgetary Reality

Incorporation of discounted cash-flow analysis provides a more realistic appraisal of trade-offs between capital-intensive replacement and incremental retrofit strategies. Discounting explicitly penalises high upfront capital expenditure, reflecting the higher near-term budgetary burden of SF_6 -free replacement relative to operational retrofits.

While discounting reduces the short-term financial attractiveness of replacement, its discounted abatement cost remains competitive due to sustained emissions elimination over the planning horizon. This supports a phased implementation logic in which retrofits address near-term stress hotspots, while replacement is pursued through dedicated capital programmes. This interpretation is consistent with established infrastructure life-cycle costing and public-sector appraisal guidance [36–38].

8.6 Maintenance Quality, Infant Mortality, and Modelling Boundaries

The framework is intentionally designed as a fleet-level screening tool rather than a unit-specific condition diagnostic model**.** While maintenance quality can cause individual older units to outperform younger neglected assets, incorporating such heterogeneity would require consistent bay-level condition-monitoring data that are not uniformly available across the fleet.

Early-life “infant mortality” associated with installation defects is a recognised phenomenon. However, in the Kuwaiti transmission context, warranty regimes and early preventive maintenance substantially suppress such effects. Fleet-level leakage behaviour is therefore dominated by mid- to late-life degradation, consistent with infrastructure reliability literature [40, 41].

8.7 Methodological Strengths and Limitations

The REE framework offers several strengths, including explicit treatment of right-censored reliability data, integration of environmental stressors, probabilistic uncertainty propagation, and planning-stage economic screening. Limitations include reliance on indirect leakage coefficients, static representation of environmental exposure, and the absence of unit-level maintenance feedback.

These limitations reflect deliberate modelling choices aligned with strategic screening rather than operational diagnostics. The framework therefore provides a transparent and extensible foundation for future work incorporating sensor-based condition monitoring, dynamic environmental inputs, and consequence-weighted decision frameworks. These findings are directly relevant to Kuwait’s national energy-transition and emissions-reduction objectives, including infrastructure modernisation targets under Kuwait Vision 2035, where prioritised replacement of high-stress assets can deliver measurable reductions in transmission-sector greenhouse-gas emissions. Taken together, these findings demonstrate that reliability-informed emissions modelling provides a defensible engineering basis for prioritising transmission-level decarbonisation investments.

9. Conclusion

This study presented an integrated Reliability–Environmental–Economic (REE) framework for evaluating ageing behaviour, environmental stress, and emissions mitigation pathways in Kuwait’s high-voltage gas-insulated switchgear (GIS) fleet. The framework combines Bayesian reliability modelling under full right-censoring with a composite environmental stress formulation and a physically grounded leakage representation, enabling probabilistic assessment of ageing-driven SF_6 emissions and comparative evaluation of mitigation scenarios under uncertainty.

Application of the framework indicates a baseline fleet-wide SF_6 leakage of approximately 6.24 t yr^{-1}, corresponding to about 1.52 × 10^5 t CO□-eq yr^{-1}. The results demonstrate that SF_6 leakage behaviour in Kuwait's transmission network arises from the combined interaction of ageing state, environmental stress, vendor and technology generation, and installed SF_6 inventory. Environmental stress alone is insufficient to explain observed emissions patterns; leakage intensification occurs primarily where elevated local stress coincides with older equipment generations and larger gas inventories. This interaction explains the concentration of emissions within a limited subset of GIS bays and substations rather than uniform fleet-wide behaviour.

Scenario analysis highlights contrasting mechanisms of emissions reduction. Measures that reduce local environmental stress primarily moderate leakage intensity and variability, whereas replacement with SF_6 -free technology structurally removes leakage pathways, resulting in lower emissions levels and narrower uncertainty envelopes over time. Quantitatively, cooling-retrofit interventions achieve moderate reductions (approximately 16–17% relative to baseline), while phased SF_6 -free replacement yields substantially larger reductions (approximately 26–31% relative to baseline) over the analysis horizon. Sensitivity analysis further indicates that emissions outcomes are governed mainly by stress amplification and SF_6 inventory, with ageing parameters exerting a secondary influence within the fully right-censored dataset.

Incorporation of discounted cash-flow analysis confirms that capital-intensive replacement strategies are more sensitive to the time value of money than operational retrofits, reflecting their higher upfront financial burden. Nevertheless, SF_6 -free replacement remains competitive on a discounted abatement-cost basis due to sustained emissions elimination over the planning horizon. These findings highlight the importance of distinguishing between short-term operational mitigation and long-term structural decarbonisation when planning transmission modernisation under budget constraints.

At the substation level, aggregation of stress-adjusted ageing, leakage potential, and contextual attributes into a composite risk index enables consistent and neutral comparison across heterogeneous assets. Although explicit consequence weighting by voltage class is not imposed, higher-voltage substations inherently exhibit larger SF_6 inventories and greater absolute emissions potential, causing them to emerge among the highest-risk assets within the screening framework. This demonstrates that system criticality is implicitly captured through physical and operational characteristics rather than imposed through arbitrary weighting.

Overall, the REE framework provides a transparent, internally consistent, and reproducible basis for analysing ageing-related emissions behaviour in hot-arid transmission systems and for comparing alternative mitigation pathways under uncertainty. The framework is intentionally designed as a fleet-level screening and prioritisation tool, rather than a unit-level diagnostic or investment-optimisation model. The findings should therefore be interpreted within the stated assumptions and scope and are intended to support comparative analysis, policy sequencing, and phased modernisation planning, rather than prescriptive asset-level decisions.

From an implementation perspective, the results translate into three operational priorities for transmission stakeholders. First, asset-management strategies should prioritise integrated ageing–environment indicators rather than chronological age alone, ensuring that replacement and retrofit decisions reflect actual stress exposure and leakage risk. Second, monitoring and intervention resources should be concentrated on high-stress substations where emissions are disproportionately concentrated, enabling targeted mitigation with measurable system-level impact. Third, transition roadmaps should combine near-term environmental hardening measures with phased deployment of SF_6 -free technologies, aligning capital planning with long-term emissions reduction trajectories and infrastructure resilience objectives.

By linking probabilistic reliability modelling with emissions estimation and economic screening, the REE framework therefore functions as a structured decision-support tool for transmission planning, supporting evidence-based prioritisation, cost-effective decarbonisation pathways, and long-horizon network reliability management.

10. Limitations and Future Research Directions

This study is subject to several limitations that arise from its scope, data structure, and intended application as a fleet-level planning tool. First, the reliability dataset is fully right-censored, as all GIS bays remain in service at the time of analysis. Consequently, Weibull ageing parameters are interpreted as relative indicators of degradation sensitivity and hazard amplification, rather than as predictors of absolute failure timing or remaining service life. This limitation is inherent to long-lived transmission assets and is explicitly addressed through Bayesian inference under full right-censoring, which permits probabilistic characterisation of ageing behaviour without requiring observed end-of-life failures.

Second, the SF_6 leakage formulation represents steady-state, ageing-driven emissions and does not explicitly resolve short-duration episodic releases or commissioning-phase effects. Scenario outcomes should therefore be interpreted as representative of medium- to long-term operational behaviour, rather than immediate post-installation or event-driven leakage dynamics, and should not be interpreted as short-term incident forecasting outputs.

Third, maintenance quality and condition-based interventions are not modelled as dynamic feedback mechanisms at the individual bay level. While vendor generation, technology cohort, and environmental stress effects are captured, the framework does not differentiate between exceptionally well-maintained older assets and poorly maintained younger units. The model is therefore intended for fleet-level screening and prioritisation, rather than unit-specific diagnostic or forensic assessment, and is not designed to replace condition-based maintenance tools or protection-system diagnostics.

The economic component of the Reliability–Environmental–Economic (REE) framework is likewise formulated as a planning-stage comparative assessment. Discounted cash-flow analysis is applied to account for the time value of money, but detailed lifecycle optimisation, financing structures, depreciation schedules, and failure-cost modelling are beyond the scope of the present study. Similarly, the composite risk index adopts equal weighting to preserve transparency and neutrality and does not encode policy-driven or consequence-based prioritisation, which should be incorporated only at downstream decision-analysis stages once screening results are obtained.

Future research will focus on extending the REE framework toward dynamic decision-support applications, including integration of online condition-monitoring data, time-varying environmental stress, maintenance feedback effects, and commissioning-phase behaviour. Additional extensions may include stochastic maintenance modelling, adaptive parameter updating using streaming sensor data, and probabilistic consequence weighting for critical substations. These extensions would enable progression from comparative screening toward full lifecycle optimisation and digital-twin–enabled asset-management planning, while preserving the probabilistic structure established in this study.

Funding and Acknowledgments

This project was fully funded by the Kuwait Foundation for the Advancement of Sciences (KFAS) under project code CN23-42SE-1891. The authors gratefully acknowledge the financial support of KFAS. The authors also thank the Department of Electrical Engineering, the laboratory facilities, and their colleagues at Australian University (AU), Kuwait, whose time and expertise were instrumental in implementing this project.

The authors express their sincere gratitude to the engineers of the Ministry of Electricity and Water (MEW), Kuwait, for their invaluable assistance in providing operational and maintenance data on gas-insulated switchgear substations. Their technical input and field insights were essential for model calibration and validation.

References

[1] H. Koch, *Gas-Insulated Transmission Lines and Substations*, Elsevier, Oxford, UK, 2022.

[2] CIGRÉ Working Group A3, Technical Brochure 849: Application of SF_6 Alternative Gases in High-Voltage Switchgear, CIGRÉ, Paris, 2021.

[3] CIGRÉ Working Group A3, Technical Brochure 871: Technical Assessment of Fluoronitrile- and Fluoroketone-Based Mixtures for HV Equipment, CIGRÉ, Paris, 2022.

[4] CIGRÉ WG A3, Technical Brochure 802: SF_6 Alternative Gases – Properties and Performance, CIGRÉ, Paris, 2021.

[5] F. Chmelik, A. Kalter, and A. Kalter, "Analysis of long-term effects during development of SF6-free gas insulated switchgear," in 27th International Conference on Electricity Distribution (CIRED 2023), Rome, Italy, 2023, pp. 2684–2688. https://doi.org/10.1049/icp.2023.1106.

[6] IPCC, *Climate Change 2021: The Physical Science Basis*, Cambridge University Press, Cambridge, UK, 2021. https://doi.org/10.1017/9781009157896.

[7] European Commission, *Proposal for a Regulation on Fluorinated Greenhouse Gases*, European Commission, Brussels, Belgium, 2022.

[8] United Nations Environment Programme (UNEP), *Fluorinated Gas Reduction Strategies*, UNEP, Nairobi, Kenya, 2022.

[9] U.S. Environmental Protection Agency, *Revised Reporting and Emissions Standards for SF_6* , U.S. EPA, Washington, DC, USA, 2023.

[10] M. S. Abu-Bakr and G. Chen, "SF6-Free Gas-Insulated Switchgear: Current Status and Future Trends," IEEE Electrical Insulation Magazine, vol. 37, no. 1, pp. 7–17, Jan.-Feb. 2021. https://doi.org/10.1109/MEI.2021.9290463.

[11] A. Al-Dousari, J. Al-Awadhi, M. Al-Rashidi, M. Ahmed, F. Al-Sharifi, Dust fallout and mineralogy in Kuwait, *J. Arid Environ.* 165 (2019) 13–23. https://doi.org/10.1016/j.jaridenv.2019.02.009.

[12] A. Al-Hemoud, et al., Economic impact of sand and dust storms in Kuwait, Econ. Disasters Clim. Change 10 (2026) 5. https://doi.org/10.1007/s41885-025-00168-1.

[13] M. Al-Rashidi, S. Al-Sabah, A. Al-Hemoud, Long-term temperature trends and extreme heat events in Kuwait, *Atmos. Res.* 267 (2022) 105993. https://doi.org/10.1016/j.atmosres.2021.105993.

[14] G. Zittis, et al., Emerging extreme heat conditions as part of the new climate normal, Theor. Appl. Climatol. 155 (2024) 143–150. https://doi.org/10.1007/s00704-023-04702-x.

[15] A. Al-Hemoud, et al., Sand and dust storm trajectories from the Mesopotamian floodplain to Kuwait, *Sci. Total Environ.* 710 (2020) 136291. https://doi.org/10.1016/j.scitotenv.2019.136291.

[16] H. Xu, B. Hu, W. Huang, X. Du, C. Shao, K. Xie, W. Li, A hybrid knowledge-based and data-driven method for aging-dependent reliability evaluation of high-voltage circuit breaker, IEEE Trans. Power Deliv. 38 (6) (2023) 4384–4396. https://doi.org/10.1109/TPWRD.2023.3277115.

[17] A. Subramaniam, S. Chandrasekar, T. Jain, Impact of thermal and humidity stress on gas-insulated switchgear ageing: A Weibull-based analysis, *IEEE Trans. Dielectr. Electr. Insul.* 28 (2) (2021) 512–521. https://doi.org/10.1109/TDEI.2021.9454532.

[18] H. Nechmi, M. Seeger, Y. Li, Alternative gas mixtures for high-voltage switchgear: Experimental validation, *IEEE Trans. Power Deliv.* 31 (3) (2016) 1340–1348. https://doi.org/10.1109/TPWRD.2015.2477799.

[19] S. Du, et al., AC breakdown and decomposition products detection characteristics of eco-friendly insulating medium in gas insulated switchgear, Sci. Rep. 14 (2024) 19491. https://doi.org/10.1038/s41598-024-70106-1.

[20] M. Seeger, H. Nechmi, Y. Li, H. Koch, Fluoroketone-based gas mixtures for high-voltage applications, *IEEE Trans. Dielectr. Electr. Insul.* 24 (6) (2017) 3734–3743. https://doi.org/10.1109/TDEI.2017.006743.

[21] CIGRÉ, *Technical Brochure 849: Application of SF_6 Alternative Gases in High-Voltage Switchgear*, CIGRÉ, Paris, France, 2021.

[22] CIGRÉ, *Technical Brochure 802: SF_6 Alternative Gases – Properties and Performance*, CIGRÉ, Paris, France, 2021.

[23] CIGRÉ, *Technical Brochure 871: Technical Assessment of Fluoronitrile- and Fluoroketone-Based Mixtures*, CIGRÉ, Paris, France, 2022.

[24] N. Zhou, Y. Xu, S. Cho, C.T. Wee, A systematic review for switchgear asset management in power grids: Condition monitoring, health assessment, and maintenance strategy, *IEEE Trans. Power Deliv.* 38 (5) (2023) 3296–3311. https://doi.org/10.1109/TPWRD.2023.3246726.

[25] R. Panmala, M. Mudaliar, H. Suryawanshi, Health-index-based condition assessment of gas-insulated switchgear under varied environmental stress, *Int. J. Electr. Power Energy Syst.* 137 (2022) 107784. https://doi.org/10.1016/j.ijepes.2021.107784.

[26] L. Yang, S. Wang, C. Chen, Q. Zhang, R. Sultana, Y. Han, Monitoring and leak diagnostics of sulfur hexafluoride and decomposition gases from power equipment for the reliability and safety of power grid operation, Appl. Sci. 14 (9) (2024) 3844. https://doi.org/10.3390/app14093844.

[27] Z. Faizol, F. Zubir, N.M. Saman, M.H. Ahmad, M.K.A. Rahim, O. Ayop, M. Jusoh, H.A. Majid, Z. Yusoff, Detection method of partial discharge on transformer and gas-insulated switchgear: A review, Appl. Sci. 13 (17) (2023) 9605. https://doi.org/10.3390/app13179605.

[28] J. Li, W. Zhou, Y. Wang, Condition monitoring and fault diagnosis of high-voltage switchgear using multi-sensor data fusion, Electr. Power Syst. Res. 213 (2022) 108399. https://doi.org/10.1016/j.epsr.2022.108399.

[29] E.D. Fylladitakis, A.X. Moronis, Design and development of a prototype operating-parameters monitoring system for high-voltage switchgear using IoT technologies, *IEEE Trans. Power Deliv.* 39 (3) (2024) 1376–1385. https://doi.org/10.1109/TPWRD.2023.3345671.

[30] M. Kuschel, et al., First F-gas-free and climate-neutral installed 420 kV GIS busducts at TransnetBW, in: *CIGRÉ Paris Session*, Paper ID 1082, 2022.

[31] A. Compare, Bayesian approaches to reliability modelling with censored data, *Reliab. Eng. Syst. Saf.* 197 (2020) 106809. https://doi.org/10.1016/j.ress.2020.106809.

[32] S. Smit, P. Heyns, A. Oberholster, Bayesian reliability updating for high-voltage equipment using incomplete lifetime data, *Electr. Power Syst. Res.* 228 (2024) 109784. https://doi.org/10.1016/j.epsr.2023.109784.

[33] H.M. Okasha, H.S. Mohammed, Y. Lio, E-Bayesian estimation of reliability characteristics of a Weibull distribution with applications, Mathematics 9 (11) (2021) 1261. https://doi.org/10.3390/math9111261.

[34] T. Liu, Y. Lio, H.M. Okasha, Reliability assessment of heavily censored data based on E-Bayesian estimation, Mathematics 10 (21) (2022) 4216. https://doi.org/10.3390/math10214216.

[35] K. Zwirglmaier, J. Straub, A. Faber, Hybrid Bayesian networks for reliability assessment of infrastructure systems, ASCE-ASME J. Risk Uncertain. Eng. Syst. Part A 10 (4) (2024) 04024019. https://doi.org/10.1061/AJRUA6.0001356.

[36] International Organization for Standardization (ISO), *ISO 15686-5:2017 Buildings and Constructed Assets, Service Life Planning, Part 5: Life Cycle Costing*, ISO, Geneva, Switzerland, 2017.

[37] International Electrotechnical Commission (IEC), *IEC 60300-3-3 Dependability Management, Part 3-3: Application Guide, Life Cycle Costing*, IEC, Geneva, Switzerland, 2017.

[38] HM Treasury, *The Green Book: Central Government Guidance on Appraisal and Evaluation*, UK Government, London, UK, 2020.

[39] M.M. Alomari, H. El-Kanj, A.-W.B. Dirawieh, N.I. Alshdaifat, A. Topal, B. Alhalaili, A multi-parameter and barrier-based approach to GIS modernization planning in Kuwait's transmission network, Proc. IEEE PES GTD Asia, Bangkok, Thailand, 2025, pp. 201–205. https://doi.org/10.1109/GTDAsia60461.2025.11313276.

[40] S. Jia, Maintenance strategy choice supported by the failure rate indicator, *Period. Polytech. Soc. Manag. Sci.* 29 (2) (2021) 165–173. https://doi.org/10.3311/PPso.17141.

[41] L. Iannacone, P. Gardoni, Modeling time-varying reliability and resilience of deteriorating infrastructure, *Reliab. Eng. Syst. Saf.* 217 (2022) 108074. https://doi.org/10.1016/j.ress.2021.108074.

Author Statement

Author Contributions

Majdi M. Alomari conceptualized the research, led the methodological framework design, contributed to the infrastructure modeling and coordinated data analysis. Ahmed Bani-Mustafa performed statistical modeling, data synthesis, and graphical outputs. Abdel-Wahab B. Dirawieh contributed to the infrastructure modeling, simulation development, and technical validation. Nafesah I. Alshdaifat conducted the literature review and supported manuscript structuring. Ayse Topal contributed to the policy analysis and stakeholder engagement design. Hania EL-Kanj performed statistical modeling, data synthesis, and graphical outputs. Badriyah Alhalaili coordinated access to national infrastructure datasets and contributed to the discussion on regulatory context. All authors contributed to writing, reviewing, and approving the final manuscript.

Funding

This project was fully funded by Kuwait Foundation for the Advancement of Sciences (KFAS) under project code CN23-42SE-1891.

Data Availability

The datasets generated and analyzed during the current study are not publicly available due to confidentiality agreements with the Ministry of Electricity, Water and Renewable Energy (MEW), but may be made available from the corresponding author upon reasonable request and with appropriate institutional permission.

Ethical Approval

Not applicable. This study did not involve human subjects or animal research.

Declaration of interests

☒ The authors declare that they have no known competing financial interests or personal relationships that could have appeared to influence the work reported in this paper.

☐ The authors declare the following financial interests/personal relationships which may be considered as potential competing interests: